







## Article

# Electrochemical Synthesis of New Isoxazoles and Triazoles Tethered with Thiouracil Base as Inhibitors of Histone Deacetylases in Human Breast Cancer Cells

Divakar Vishwanath <sup>1</sup>, Zhang Xi <sup>2</sup>, Akshay Ravish <sup>1</sup>, Arunkumar Mohan <sup>1</sup>, Shreeja Basappa <sup>3</sup>, Niranjan Pattehalli Krishnamurthy <sup>4</sup>, Santosh L. Gaonkar <sup>5</sup>, Vijay Pandey <sup>6,7</sup>, Peter E. Lobie <sup>2,6,7,\*</sup> and Basappa Basappa <sup>1,\*</sup>

- <sup>1</sup> Laboratory of Chemical Biology, Department of Studies in Organic Chemistry, University of Mysore, Mysore 570006, Karnataka, India; divakardivi166@gmail.com (D.V.); akshayrv533@gmail.com (A.R.); arunmysore3@gmail.com (A.M.)
- <sup>2</sup> Shenzhen Bay Laboratory, Shenzhen 518055, China; zhangxi@szbl.ac.cn
- <sup>3</sup> Department of Chemistry, BITS–Pilani Hyderabad Campus, Jawaharnagar 500078, Medchal, Telangana, India; f20210833@hyderabad.bits-pilani.ac.in
- <sup>4</sup> NMR Research Centre, Indian Institute of Science, Bangalore 560012, Karnataka, India; niranjanursa@gmail.com
- <sup>5</sup> Department of Chemistry, Manipal Institute of Technology, Manipal Academy of Higher Education, Manipal 576104, Karnataka, India; sl.gaonkar@manipal.edu
- <sup>6</sup> Tsinghua Berkeley Shenzhen Institute, Tsinghua Shenzhen International Graduate School, Tsinghua University, Shenzhen 518055, China; vijay.pandey@sz.tsinghua.edu.cn
- <sup>7</sup> Institute of Biopharmaceutical and Health Engineering, Tsinghua Shenzhen International Graduate School, Tsinghua University, Shenzhen 518055, China
- \* Correspondence: pelobie@sz.tsinghua.edu.cn (P.E.L.); salundibasappa@gmail.com (B.B.)



**Citation:** Vishwanath, D.; Xi, Z.; Ravish, A.; Mohan, A.; Basappa, S.; Krishnamurthy, N.P.; Gaonkar, S.L.; Pandey, V.; Lobie, P.E.; Basappa, B. Electrochemical Synthesis of New Isoxazoles and Triazoles Tethered with Thiouracil Base as Inhibitors of Histone Deacetylases in Human Breast Cancer Cells. *Molecules* **2023**, *28*, 5254. <https://doi.org/10.3390/molecules28135254>

Academic Editors: Alejandro Samhan-Arias and Carmen Sanmartín

Received: 16 April 2023

Revised: 11 June 2023

Accepted: 12 June 2023

Published: 6 July 2023



**Copyright:** © 2023 by the authors. Licensee MDPI, Basel, Switzerland. This article is an open access article distributed under the terms and conditions of the Creative Commons Attribution (CC BY) license (<https://creativecommons.org/licenses/by/4.0/>).

**Abstract:** Histone deacetylases (HDACs) are an attractive drug target for the treatment of human breast cancer (BC), and therefore, HDAC inhibitors (HDACis) are being used in preclinical and clinical studies. The need to understand the scope of the mode of action of HDACis, as well as the report of the co-crystal structure of HDAC6/SS-208 at the catalytic site, provoked us to develop an isoxazole-based lead structure called 4-(2-(((1-(3,4-dichlorophenyl)-1H-1,2,3-triazol-4-yl)methyl)thio)pyrimidin-4-yl)morpholine (**5h**) and 1-(2-(((3-(p-tolyl) isoxazol-5-yl)methyl)thio)pyrimidin-4-yl)piperidin-4-one (**6l**) that targets HDACs in human BC cells. We found that the compound **5h** or **6l** could inhibit the proliferation of BC cells with an IC<sub>50</sub> value of 8.754 and 11.71 μM, respectively. Our detailed *in silico* analysis showed that **5h** or **6l** compounds could target HDAC in MCF-7 cells. In conclusion, we identified a new structure bearing triazole, isoxazole, and thiouracil moiety, which could target HDAC in MCF-7 cells and serve as a base to make new drugs against cancer.

**Keywords:** breast cancer; HDAC; triazole; isoxazole; thiouracil; drug discovery; cell viability assay; molecular docking

## 1. Introduction

Histone deacetylases (HDACs) remove acetyl groups from lysine residues on acetylated histones, leading to changes in chromatin structure and gene expression. In breast cancer (BC), HDACs were found to be overexpressed and regulate the expression of a tumor-suppressor gene called BRCA1, which was involved in DNA repair, cell-cycle control, and cancer-cell progression [1–4]. In addition, HDACs play an essential role in oncogenic pathways, such as the estrogen-receptor (ER) signaling pathway, which leads to ER-positive BC [5]. Structurally, the catalytic site of HDACs contains four regions of highly conserved amino acids, where the first region is referred to as a zinc-binding domain, which is coordinated by two histidines and one aspartic acid residue [6–8]. The second region was known as the catalytic triad (His-Asp-Tyr) domain, which consists of three amino acid

residues involved in the deacetylation reaction [9]. Moreover, the active site of HDACs contains a hydrophobic pocket region with phenylalanine and tyrosine-rich amino acids that bind to the histone substrate's acetyl group [10]. Finally, the catalytic site of HDACs has a lysine binding domain composed of asparagine, glutamic acid, and leucine amino acids, which were found to interact with the  $\epsilon$ -amino group of the lysine residue on the histone substrate [11].

In recent years, HDACs have emerged as promising drug targets for treating cancer and other neurological diseases [12]. HDAC inhibitors mainly modulate gene expressions and induce apoptosis and cell differentiation; therefore, HDACs are promising drug targets. The HDAC inhibitors (HDACis) were broadly subclassified into four classes called hydroxamic acids, short-chain fatty acids, cyclic peptides, and benzamides, and the US FDA approved some of them for the treatment of patients. Vorinostat, Belinostat, Panobinostat, Givinostat, Trichostatin A, Scriptaid, JNJ-26481585, MC1568, MC-1293, and ACY-1215 are the drugs bearing hydroxamic acid in their chemical structure [13–21]. HDACis, like valproic acid and sodium butyrate, fall under the short-chain fatty acids class, while Romidepsin, Apicidin, and Lagazole Thiol fall under cyclic peptides [13,22]. Mocetinostat, CI-994, RGFP966, Tubastatin A, and TMP195 are a few HDACis from the benzamide category [13,23–25].

In this regard, we previously demonstrated that the lead compound 3-(4-(4-phenoxyphenyl)-1*H*-1,2,3-triazol-1-yl)benzo[*d*]isoxazole (**1**) targeted histone deacetylases in cancer cells, which displayed a high degree of shape complementarity to the binding site of the enzyme [26]. Triazole-based carboxamides, such as the SAHA analog (**2**), exhibited potent inhibitory activity towards HDAC8 and were shown to be a potential anticancer agent and induce antitumor effects in preclinical studies [27].

The potent molecule with a thiouracil core, like (*E*)-*N*-hydroxy-3-(4-(((6-oxo-4-phenyl-1,6-dihydropyrimidin-2-yl)thio)methyl)phenyl)acrylamide (**3**), selectively inhibited HDAC1 (class I) activity in a cell-based assay [28]. Additionally, the studies on thiouracil-based compounds such as compound (**4**) were found to be the most potent and class I-selective HDACi of the tested series, exhibiting anticancer activity [29].

In addition, the co-crystal structure of HDAC6 and an anticancer molecule called isoxazole-3-hydroxamate (**5**) complex revealed that it is bound to the zinc-binding domain and a nearby hydrophobic region [30]. Another isoxazole-based derivative 5-(3-bromo-4-hydroxyphenyl)-3-(thiophene-2-yl) isoxazole (**6**) showed an anticancer effect by acting as an HDAC inhibitor [31].

Based on our laboratory results on the triazole–isoxazole hybrid structure and the role of substitute thiouracil on HDACis role, we designed a novel structure and developed an extensive library of compounds that could serve as a base to develop new drugs that target HDAC in BC (Figures 1 and 2).

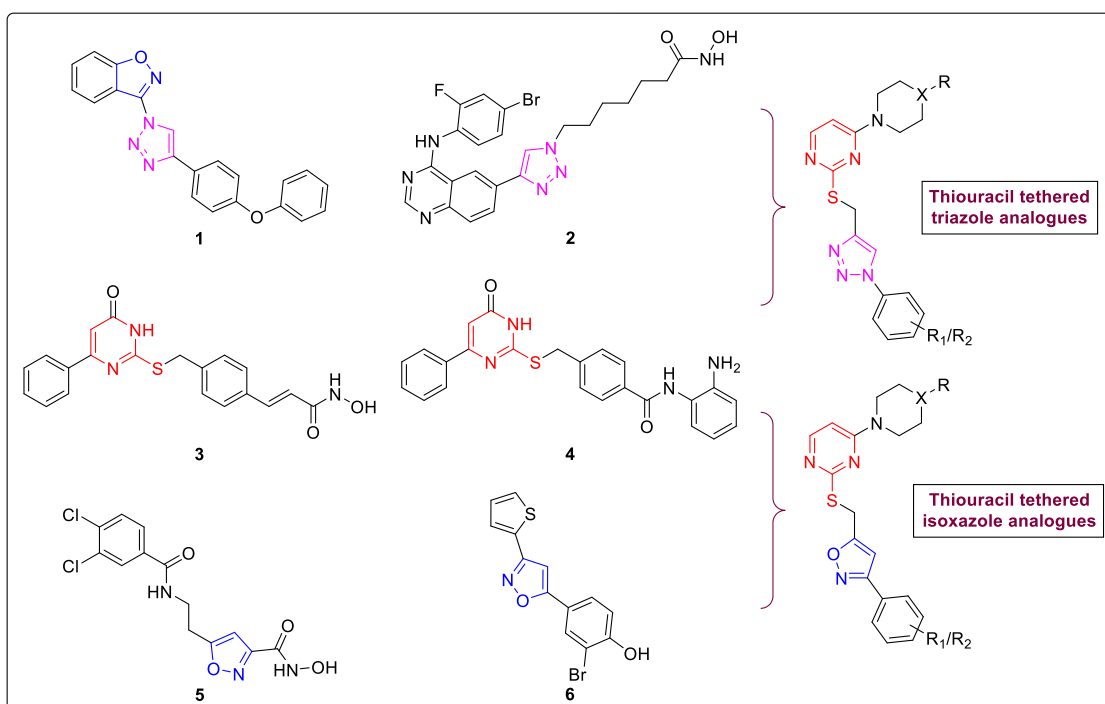


**Figure 1.** Evolution of HDACis based on a hybrid structure bearing triazole or isoxazole and thiouracil-based core heterocycles; Structures 1 and 2 represents 1,2,3-triazoles (pink), 3 and 4 represents thiouracil (red) analogues also 5 and 6 represents isoxazole (blue) derivatives as HDACis inhibitors.

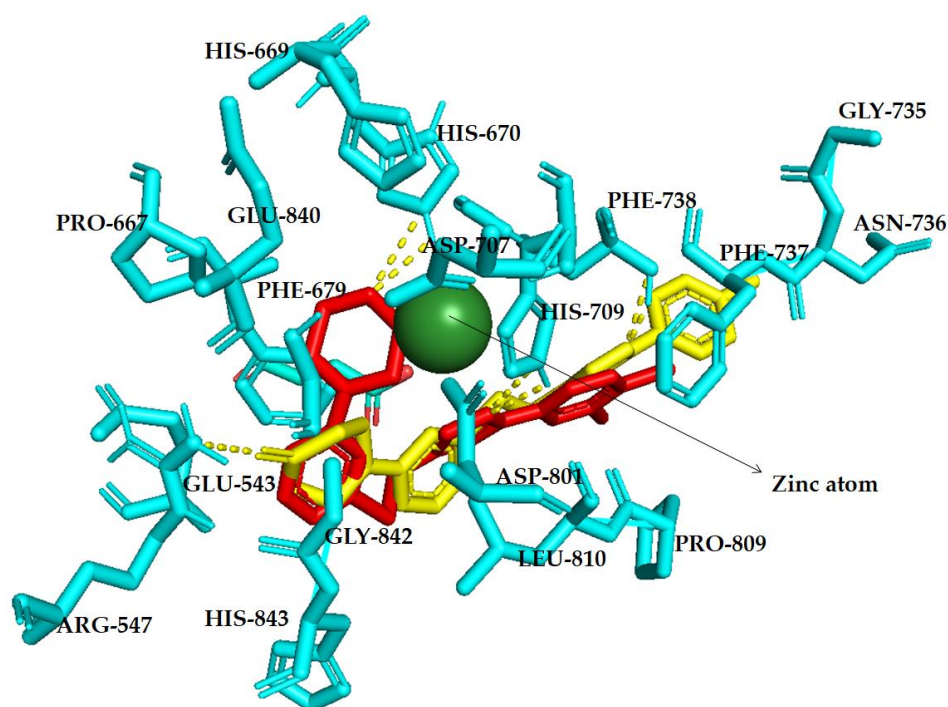
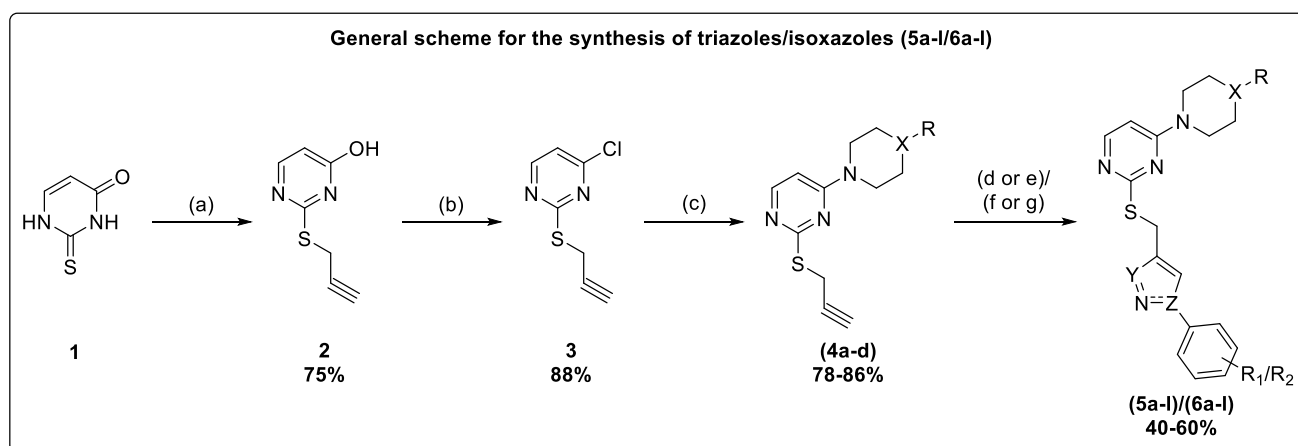


**Figure 2.** The docked lead triazole (5h; red) and lead isoxazole (6l; yellow) were visually represented in a detailed stick form, showing their evolution as HDACis on the isoxazole and triazole scaffold. The HDAC (cyan-HDAC7) active site, which contains zinc ( $Zn^{2+}$ , green), was the target of these compounds. Within the active site is a zinc-binding site and two Asp residues (Asp801–Asp707). The walls of the pocket are lined with hydrophobic residues (Pro667, Phe679, Phe737, Phe738, Pro809 and Leu810), while other residues present include His709, His670, ARG547, Gly842 and others. Dotted lines (yellow) represents hydrogen bondings.

## 2. Results and Discussion

### 2.1. Synthesis of Thiouracil Tethered Triazole/Isoxazole Analogues

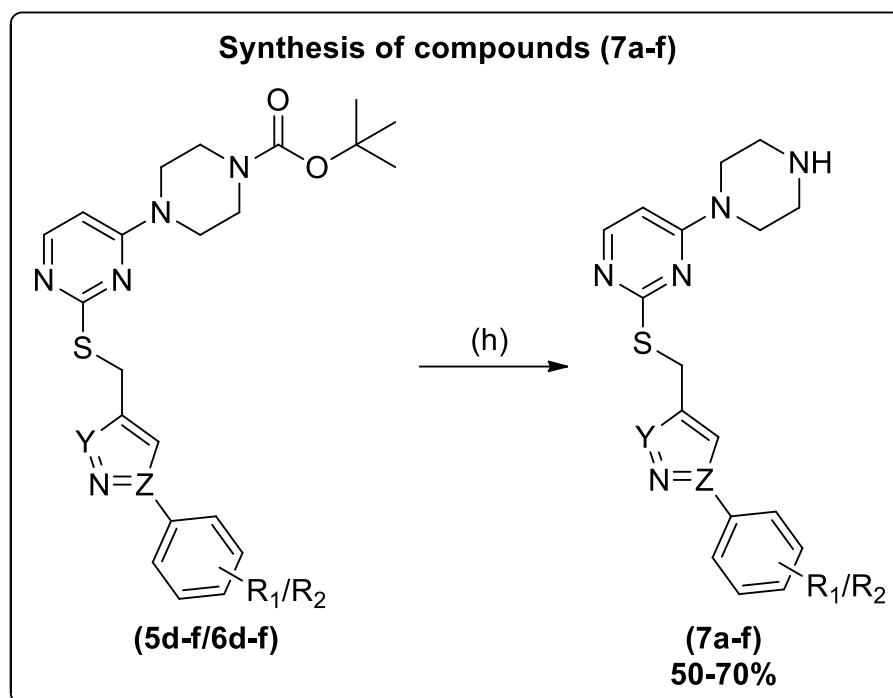
The present work synthesized novel thiouracil-tethered triazole/isoxazole derivatives and studied their anticancer activity. Triazole analogues (**5a–l**) were obtained by adding CuI to a stirred solution of substituted azides and intermediates (**4a–d**) in THF under basic conditions. Additionally, the synthesis of 1,2,3-triazoles was performed via electrochemical oxidation of copper foil cells as the working electrode and platinum as the counter electrode in tertiary butanol:water medium (1:1). The reaction gave a good yield in the presence of an analytical amount of tetrabutylammonium tetrafluoroborate (TBATFB) within 60 min. This method was highly useful for synthesizing 1,2,3-triazoles tethered with a bioactive scaffold (Scheme 1).



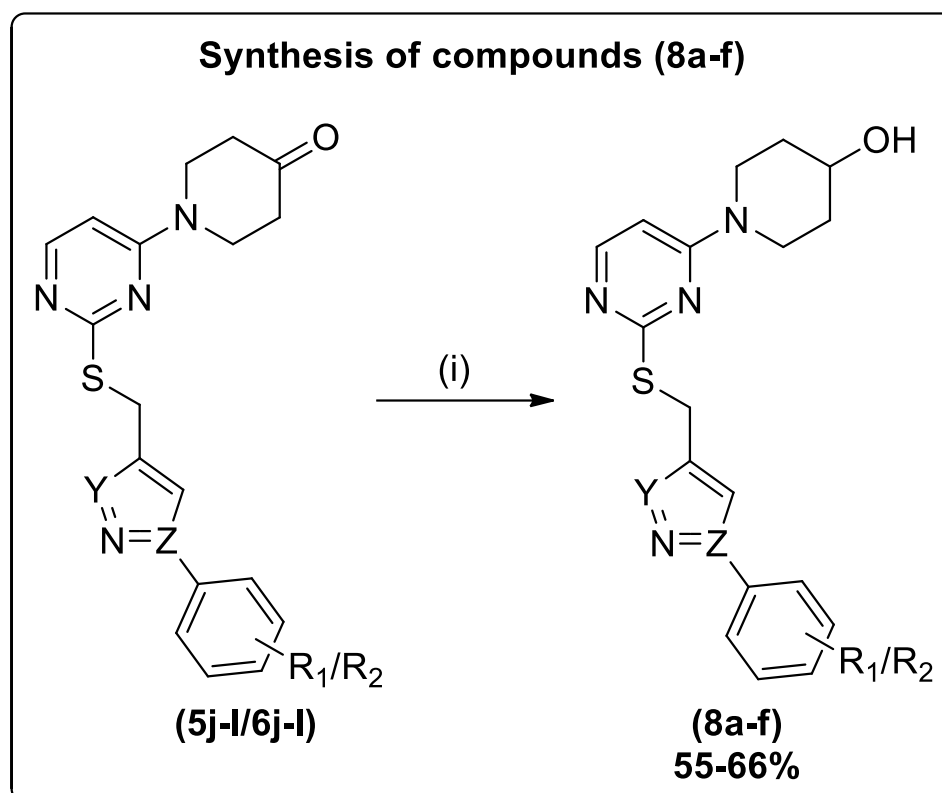
**Scheme 1.** Reagents and conditions: (a) propargyl bromide, KOH, EtOH:H<sub>2</sub>O (1:1), reflux at 50 °C, 45 min; (b) POCl<sub>3</sub>, reflux, 20 min; (c) substituted piperazines/morpholine/4-piperidinone, acetone, Et<sub>3</sub>N, reflux, 8–10 h; (d) substituted phenyl azides, CuI, THF, Et<sub>3</sub>N, r.t., 3–5 h; (e) Cu foil and Pt electrodes, *tert*-butyl alcohol/water (1:1), tetrabutylammonium tetrafluoroborate, electrolysis; (f) *N*-hydroxy-(substituted) benzimidoyl chloride, DMF, Et<sub>3</sub>N, 0-r.t.; (g) Pt and Fe electrodes, MeOH, electrolysis.

Isoxazole analogues (**6a–l**) were obtained via a cyclization reaction between *N*-hydroxy-(substituted) benzimidoyl chloride and intermediates (**4a–d**) in DMF under basic conditions. Moreover, the synthesis of isoxazole was conducted using the electrolysis method. Under constant current supplying with a density of 5.0 mA/cm<sup>−2</sup> into a beaker-type undivided cell, *N*-hydroxy-(substituted) benzimidoyl chlorides and alkynes (**4a–d**) were reacted by using Pt-plate as the working electrode and an iron rod as the cathode in methanolic medium, and the desired isoxazoles were obtained in good yield when compared to the abovementioned conventional method (Scheme 1).

Furthermore, the *N*-*boc* deprotection of compounds (**5d–f/6d–f**) was accomplished upon treatment with trifluoroacetic acid in DCM to yield (**7a–f**) (Scheme 2). The ketone group reduction in compounds (**5j–l/6j–l**) was made on treatment with sodium borohydride in THF to yield (**8a–f**) (Scheme 3).



**Scheme 2.** Reagents and conditions: (h) (5d-f/6d-f), DCM, CF<sub>3</sub>COOH, r.t., 1 h.

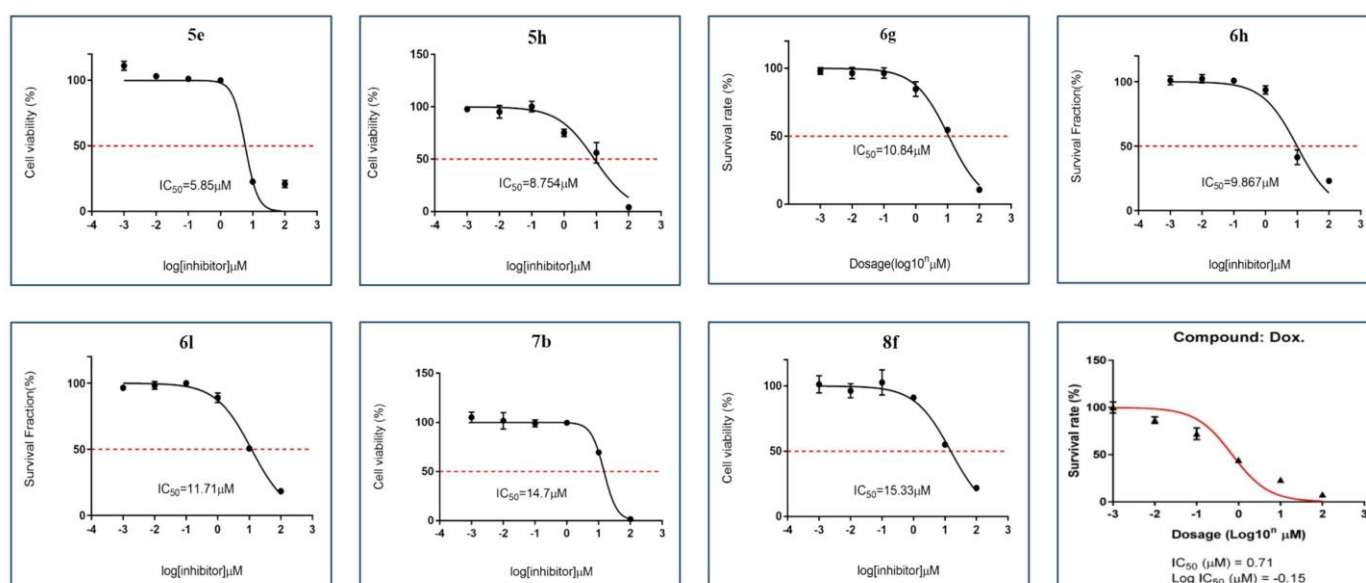


**Scheme 3.** Reagents and conditions: (i) (5j-l/6j-l), THF, NaBH<sub>4</sub>, r.t., 1.5 h.

## 2.2. Cytotoxicity of Thiouracil Tethered Triazole/Isoxazole Analogues on MCF-7 Cells

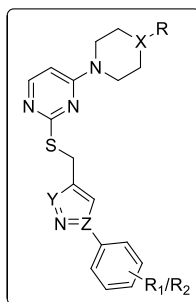
Initially, the novel thiouracil tethered triazole/isoxazole analogues were subjected to cell viability studies against human breast cancer (BC) (MCF-7) cells (Table 1), using the Alamar Blue assay [32–34]. For over four decades, numerous research groups have extensively utilized MCF-7, a BC cell line exhibiting a well-characterized molecular profile

and dependence on estrogen, in drug development research [35,36]. The assay was performed at different concentrations (0, 0.01, 0.1, 1, 10, or 100  $\mu\text{M}$ ) for 72 h, and the positive control Doxorubicin inhibited the viability of MCF-7 cells with an  $\text{IC}_{50}$  value of 0.71  $\mu\text{M}$ . The results of the assay displayed that compounds **5e**, **5h**, **6g**, **6h**, **6l**, **7b**, or **8f** produced loss of viability of MCF-7 cells with varied  $\text{IC}_{50}$  values of 5.85, 8.754, 10.84, 9.867, 11.71, 14.70, or 15.33  $\mu\text{M}$ , respectively (Figure 3). In addition, the active compounds are non-toxic to immortalized breast cancer cells (MCF-10A) (Supplementary Materials). Among the tested isoxazole and triazole-tethered thiouracil molecules, triazole-based compounds bearing 3,4-dichloro phenyl group in **5c**, **5e**, **5h**, or **7b** inhibited the human BC cells with an  $\text{IC}_{50}$  value of 11.31, 5.85, 8.754, or 14.7  $\mu\text{M}$ , respectively, when compared to less active compounds that belonged to methoxy, methyl, or hydroxy-phenyl groups. Moreover, in isoxazoles molecules, those bearing methoxyphenyl-substitution in compounds **6d**, **6h**, **6g**, or **7d** were found to be cytotoxic to human BC cells, with  $\text{IC}_{50}$  values of 15.96, 10.84, 9.86, or 14.8  $\mu\text{M}$ , respectively. On the other hand, methylphenyl-substitution-to-isoxazole-based compounds such as **6i**, **6l**, **7f**, or **8f** showed considerable  $\text{IC}_{50}$  values of 43.27, 11.71, 14.83, or 15.33  $\mu\text{M}$ , respectively. So, the SAR data revealed that the compounds having triazole and 3,4-dichloro phenyl substitutions favored higher cytotoxicity. In contrast, the isoxazole compound and methoxy or methyl-phenyl-substitution showed better bioactivity against human BC cells.



**Figure 3.** Effect of lead compounds **5e**, **5h**, **6g**, **6h**, **6l**, **7b**, and **8f** on MCF7 cell viability (black line), as determined by the Alamar Blue cell viability assay, with Doxorubicin as positive control (red line), as described in the Materials and Methods section. Error bars represent SD, and points (0, 0.01, 0.1, 1, 10, or 100  $\mu\text{M}$ ) represent the mean of three independent measurements after 72 h incubation of compounds. Error bars indicate an SD of 2.3. In Silico molecular interaction studies of compounds bearing isoxazole (**6l**) and triazole (**5h**) on HDAC7.

We previously reported that the isoxazole-and-triazole-bearing group targets HDAC, which showed a similar binding pattern of HDACis at the active site of an enzyme and formed multiple molecular interactions in the hydrophobic region [26]. In continuation of development of new HDACis, we carried out the molecular docking analysis of lead structures (**6l**) 1-(2-(((3-(*p*-tolyl) isoxazol-5-yl)methyl)thio) pyrimidin-4-yl) piperidin-4-one and (**5h**) 4-(2-(((1-(3,4-dichlorophenyl)-1*H*-1,2,3-triazol-4-yl)methyl)thio) pyrimidin-4-yl) morpholine, using the co-crystal structure of HDAC7 (PDB ID: 3ZNR), which bound to the isoxazole and triazole ligands, respectively.

**Table 1.** List of compounds synthesized.

Compound Code	X,Y,Z	R	R <sub>1</sub> /R <sub>2</sub>	MCF-7/IC <sub>50</sub> (μM)
5a	N,N,N	2,3-Cl <sub>2</sub> C <sub>6</sub> H <sub>3</sub>	4-OCH <sub>3</sub>	>100
5b	N,N,N	2,3-Cl <sub>2</sub> C <sub>6</sub> H <sub>3</sub>	3,4-Cl <sub>2</sub>	>100
5c	N,N,N	2,3-Cl <sub>2</sub> C <sub>6</sub> H <sub>3</sub>	4-OH	11.31
5d	N,N,N	COOC(CH <sub>3</sub> ) <sub>3</sub>	4-OCH <sub>3</sub>	26.59
5e	N,N,N	COOC(CH <sub>3</sub> ) <sub>3</sub>	3,4-Cl <sub>2</sub>	5.85
5f	N,N,N	COOC(CH <sub>3</sub> ) <sub>3</sub>	4-OH	24.12
5g	O,N,N	-	4-OCH <sub>3</sub>	>100
5h	O,N,N	-	3,4-Cl <sub>2</sub>	8.754
5i	O,N,N	-	4-OH	>100
5j	C,N,N	O	4-OCH <sub>3</sub>	16.14
5k	C,N,N	O	3,4-Cl <sub>2</sub>	30.10
5l	C,N,N	O	4-OH	23.20
6a	N,O,C	2,3-Cl <sub>2</sub> C <sub>6</sub> H <sub>3</sub>	4-OCH <sub>3</sub>	66.09
6b	N,O,C	2,3-Cl <sub>2</sub> C <sub>6</sub> H <sub>3</sub>	3,4-(OCH <sub>3</sub> ) <sub>2</sub>	28.39
6c	N,O,C	2,3-Cl <sub>2</sub> C <sub>6</sub> H <sub>3</sub>	4-CH <sub>3</sub>	>100
6d	N,O,C	COOC(CH <sub>3</sub> ) <sub>3</sub>	4-OCH <sub>3</sub>	15.96
6e	N,O,C	COOC(CH <sub>3</sub> ) <sub>3</sub>	3,4-(OCH <sub>3</sub> ) <sub>2</sub>	>100
6f	N,O,C	COOC(CH <sub>3</sub> ) <sub>3</sub>	4-CH <sub>3</sub>	19.84
6g	O,O,C	-	4-OCH <sub>3</sub>	10.84
6h	O,O,C	-	3,4-(OCH <sub>3</sub> ) <sub>2</sub>	9.867
6i	O,O,C	-	4-CH <sub>3</sub>	43.27
6j	C,O,C	O	4-OCH <sub>3</sub>	26.90
6k	C,O,C	O	3,4-(OCH <sub>3</sub> ) <sub>2</sub>	33.35
6l	C,O,C	O	4-CH <sub>3</sub>	11.71
7a	N,N,N	H	4-OCH <sub>3</sub>	>100
7b	N,N,N	H	3,4-Cl <sub>2</sub>	14.7
7c	N,N,N	H	4-OH	>100
7d	N,O,C	H	4-OCH <sub>3</sub>	14.83
7e	N,O,C	H	3,4-(OCH <sub>3</sub> ) <sub>2</sub>	>100
7f	N,O,C	H	4-CH <sub>3</sub>	28.94
8a	C,N,N	OH	4-OCH <sub>3</sub>	>100
8b	C,N,N	OH	3,4-Cl <sub>2</sub>	30.26
8c	C,N,N	OH	4-OH	>100
8d	C,O,C	OH	4-OCH <sub>3</sub>	21.87
8e	C,O,C	OH	3,4-(OCH <sub>3</sub> ) <sub>2</sub>	19.38
8f	C,O,C	OH	4-CH <sub>3</sub>	15.33
Doxorubicin	0.71			



We initially retrieved HDAC7 co-crystal structure from RCSB PDB (PDB ID: 3ZNR) and used it for docking purposes [37]. The Scripps Research Institute's Auto-Dock4 tools (ADT)v1.5.6 was used for docking. The protein structure HDAC7, compounds **6l** and **5h**, and co-crystal ligand (TMP269) were prepared using discovery studio BIOVIA Discovery Studio 2021 client and Avogadro, and later it was docked using AutoDock tools (ADT).

The isoxazole derivative (**6l**) exhibited a binding energy of  $-6.60$  kcal/mol, indicating a strong affinity for the HDAC7 binding site. Similarly, the triazole derivative (**5h**) demonstrated a slightly higher binding energy of  $-6.42$  kcal/mol, suggesting an even more robust interaction with the target protein. Both compounds displayed favourable binding energies, indicating their potential as HDAC7 inhibitors, and cartoon representations of docked compounds are depicted in Figure 4A,B. In comparison, the co-crystal ligand (TMP269) exhibited a binding energy of  $-6.19$  kcal/mol, which falls within the range of the isoxazole and triazole compounds. This suggests that the co-crystal ligand also possesses a significant binding affinity for HDAC7.

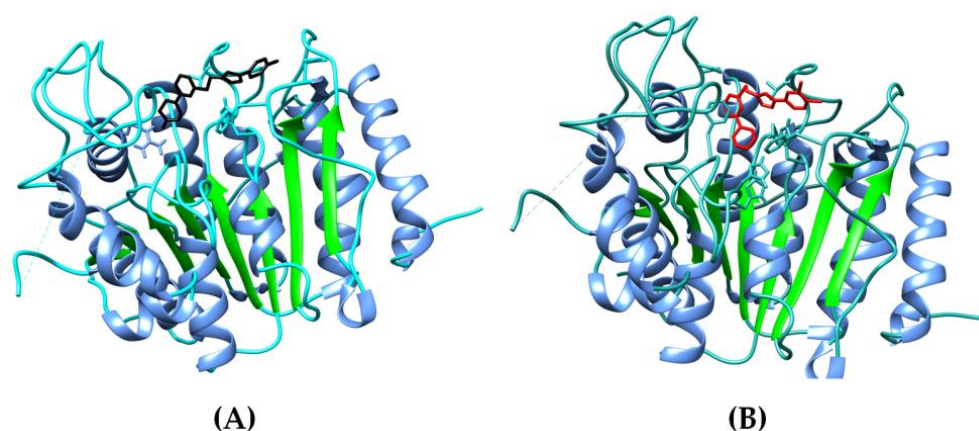


**Figure 4.** Cartoon representation of docked compounds **6l** (black) (A) and **5h** (red) (B) towards the active site of HDAC7.

An analysis of the binding pocket revealed critical interactions for the isoxazole, triazole, and co-crystal ligands. The isoxazole compound (**6l**) formed hydrogen bonds with residue PHE-738 with a bond distance of  $1.83$  Å, stabilizing its binding within the pocket (Figure 5A). Moreover, **6l** had  $\pi$ -sigma bond formation with the residue LEU-810 with a bond distance of  $3.65$  Å, and  $\pi$ - $\pi$  T-shaped bonds formed with residue PHE-738 with a bond distance of  $5.63$  Å, and alkyl bond formed with residues LEU-810 and PRO-542, respectively. The triazole compound (**5h**) displayed hydrogen bond interactions with residue HIS-709 having a bond distance of  $2.69$  Å, and  $\pi$ -alkyl bonds were formed with residues PRO-242, HIS-670, PHE-679, PHE-737, PRO-809, and LEU-810, contributing to its strong binding (Figure 5B). The co-crystal ligand (TMP269) demonstrated hydrogen bond interactions with residues PHE-738 with a bond distance of  $2.36$  Å, and a  $\pi$ -alkyl bond formed with residues HIS-709 and PHE-738 with bond distances of  $5.43$  Å and  $4.73$  Å, respectively. Furthermore, TMP269 had a  $\pi$ -sigma bond and salt bridge interactions with residues LEU-810 and ASP-626, respectively (Figure 5C). These interactions play a crucial role in maintaining the stability and specificity of the ligand-protein complex.

The results of the molecular docking study highlight the good binding affinity of both the isoxazole (**6l**) and triazole (**5h**) compounds towards the HDAC7 binding site, with binding energies of  $-6.60$  and  $-6.42$  kcal/mol, respectively. These findings suggest that both compounds have the potential to be effective inhibitors of HDAC7. Furthermore, the co-crystal ligand (TMP269) exhibited a favourable binding energy of  $-6.19$  kcal/mol, indicating its potency as an HDAC7 inhibitor. The critical interactions observed within the binding pocket emphasize the role of specific residues in facilitating ligand-protein interactions for all three compounds.



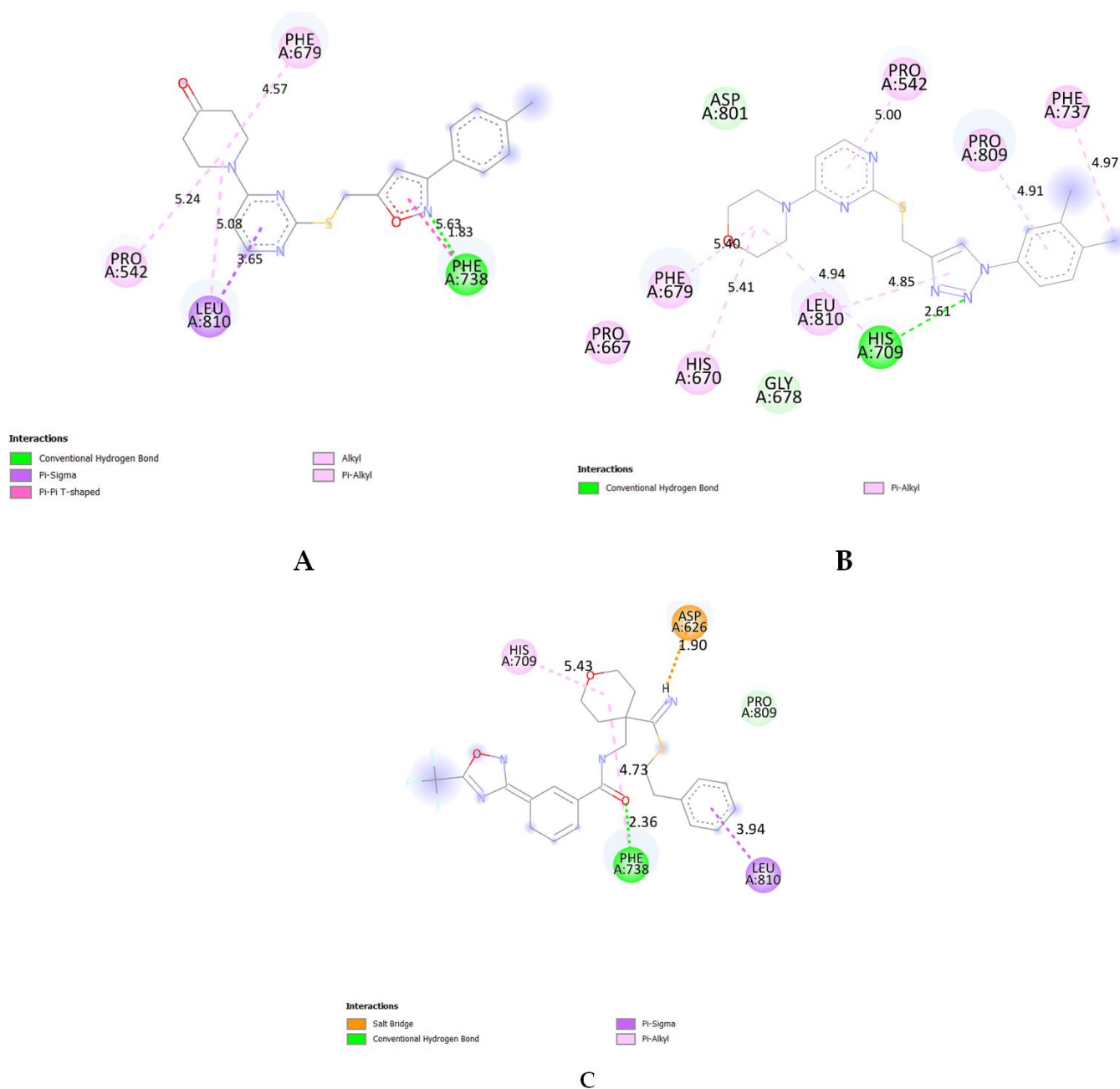


**Figure 5.** Representation of 2D structures of compounds **6l** (A), **5h** (B), and co-crystal ligand (TMP269) (C) interacting with the active site of HDAC7 (PDB ID: 3ZNR). Dotted lines represents bond distances.

These results provide valuable insights into the potential therapeutic utility of the isoxazole (**6l**) and triazole (**5h**) compounds as HDAC7 inhibitors—also, the 3D surface view of **6l** and **5h** is represented in Figure 6.

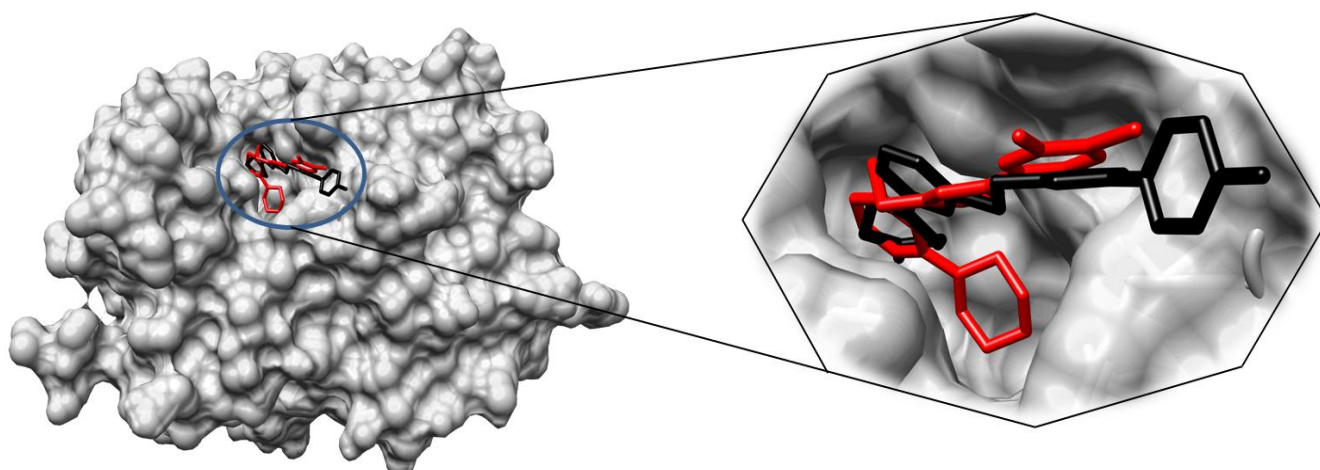


**Figure 6.** Three-dimensional surface image and its enlarged view of docked compounds **6l** (black) and **5h** (represented in red color) with active site groove of HDAC7.

### 3. Materials and Methods

All chemicals and solvents were purchased from Sigma-Aldrich (Bangalore, India). Pre-coated silica gel TLC plates monitored the completion of the reaction. An Agilent mass spectrophotometer was used to record the mass of the synthesized compounds.  $^1\text{H}$  and  $^{13}\text{C}$  NMR were recorded on Bruker (400 MHz) and Jeol NMR spectrophotometers (500 MHz). TMS was used as an internal standard, and deuterated DMSO and chloroform were used as solvents. Chemical shifts are expressed as ppm.

#### 3.1. General Procedure for the Synthesis of Intermediates (4a–d)

Potassium hydroxide (1.4 mmol) was dissolved in ethanol:water (1:1) in an RB flask, and 2-thiouracil (**1**) (1 mmol) was added. After 5 min, propargyl bromide (1.5 mmol) was added and refluxed at 50 °C for 45 min. The completion of the reaction was monitored by TLC (EtOAc:Hexane) (3:7), and ethanol was evaporated under high vacuum pressure. The crude was washed with 10% bicarbonate solution, ethanol, and diethyl ether to yield pure 2-(prop-2-yn-1-ylthio) pyrimidin-4-ol (**2**) [38]. Reactant (**2**) was refluxed in  $\text{POCl}_3$  for 20 min after completion of the reaction [TLC: (EtOAc:Hexane) (1:9)]; the reaction mixture was quenched in ice-cold water and neutralized by potassium carbonate [39]. Then, the reaction mass was extracted to the ethyl acetate layer and concentrated using a rotary evaporator to afford 4-chloro-2-(prop-2-yn-1-ylthio)pyrimidine (**3**). For Compound (**3**) (1 mmol), substituted piperazines/morpholine/4-piperidinone (1 mmol) were dissolved in acetone and refluxed in the presence of base triethylamine ( $\text{Et}_3\text{N}$ ) (2 mmol) for 8–10 h [40]. TLC was monitored for the completion of the reaction, and the crude intermediates (**4a–d**) were purified by column chromatography (EtOAc:Hexane) (2:8) (Scheme 1).

#### 3.2. General Procedure for the Synthesis of Thiouracil Tethered Triazoles (5a–l)

A. Conventional method: To a stirred solution of substituted azides (1.2 mmol), (**4a–d**) (1 mmol) in tetrahydrofuran (THF), CuI (20 mol%), and triethylamine (2.0 mmol) was added, and the reaction mixture was stirred at room temperature for 3–5 h. After completion of the reaction [TLC: (EtOAc:Hexane) (4:6)], THF was distilled off, and the crude was purified by column chromatography to afford thiouracil tethered triazole derivatives (**5a–l**) (Scheme 1) [41].

B. Electrochemical method: In the presence of copper (Cu) foil and platinum (Pt) electrodes, the azides and alkynes dissolved in *tert*-butyl alcohol and water (1:1) medium were subjected to a 0.3 voltage of current in the catalytic amount of TBATFB (0.1 mmol) for 1 h. The reaction was monitored by TLC [(EtOAc:Hexane) (4:6)], and soon after the completion of the reaction, the 1,2,3-triazoles were extracted in ethyl acetate and purified using column chromatography (Scheme 1).

### 3.3. General Procedure for the Synthesis of Thiouracil Tethered Isoxazoles (6a–l)

A. Conventional method: To a stirred solution of *N*-hydroxy-(substituted)benzimidoyl chloride (1 mmol) in dimethylformamide (DMF), triethylamine (2.5 mmol) was added slowly at 0–4 °C. After 10 min, compound (4a–d) was added and stirred overnight at room temperature. After completion of the reaction TLC: (EtOAc:Hexane) (3:7), water was added to the above reaction mixture, and the crude obtained was filtered. The crude was purified by column chromatography to yield pure thiouracil tethered isoxazole derivatives (6a–l) (Scheme 1) [42].

B. Electrochemical method: Beaker-type undivided cells containing platinum (Pt) and iron (Fe) rod as electrodes and methanol as media were kept at room temperature. *N*-hydroxy-(substituted) benzimidoyl chlorides and alkynes were added to the solution, and the current 5.0 mA/cm<sup>−2</sup> was passed to the reaction mixture. The reaction was stirred for 60 min under stirring, and the reaction was monitored by TLC [(EtOAc:Hexane) (3:7)] and was terminated when the substrate was consumed. The products were isolated as mentioned in the abovementioned procedure (Scheme 1).

### 3.4. General Procedure for the Synthesis of Compounds (7a–f)

To a stirred solution of compounds (5d–f/6d–f) in dichloromethane (DCM), 0.5 mL of trifluoroacetic acid was added slowly at 0–4 °C, and the reaction mixture was stirred at room temperature for 1 h [43]. After completion of the *N*-*boc* deprotection [TLC: (MeOH:EtOAc) (1:9)], the solvent was distilled off using a rotary evaporator. The residues were neutralized by a 20% K<sub>2</sub>CO<sub>3</sub> solution, extracted with an ethyl acetate layer, and dried over Na<sub>2</sub>SO<sub>4</sub>. Then, ethyl acetate was concentrated in a rotary evaporator and recrystallized with the appropriate solvent to afford the target compounds (7a–f) (Scheme 2).

### 3.5. General Procedure for the Synthesis of Compounds (8a–f)

To a stirred solution of compounds (5j–l/6j–l) (1 mmol) in THF, sodium borohydride (1.2 mmol) was added, and the reaction mass was stirred at room temperature for 1.5 h. After completion of ketone group reduction [TLC: (EtOAc: Hexane) (7:3)], the solvent was distilled off using a rotary evaporator. The residues were neutralized by the slow addition of water, extracted with an ethyl acetate layer, and dried over Na<sub>2</sub>SO<sub>4</sub>. Then, ethyl acetate was distilled off, and the crude was purified through column chromatography or recrystallized with the appropriate solvents to afford the final compounds (8a–f) (Scheme 3).

### 3.6. 4-Chloro-2-(prop-2-yn-1-ylthio)pyrimidine (3)

LCMS (ESI): *m/z* calcd. for C<sub>7</sub>H<sub>5</sub>ClN<sub>2</sub>S: 184.6460, found = 185.0446 [M + H]<sup>+</sup>, 187.0405 [M + 2H]<sup>+</sup>.

### 3.7. 4-(4-(2,3-Dichlorophenyl) piperazin-1-yl)-2-(((1-(4-methoxyphenyl)-1H-1,2,3-triazol-4-yl)methyl)thio) pyrimidine (5a)

Off-white solid; 55% yield; mp: 154–156 °C; <sup>1</sup>H NMR (CDCl<sub>3</sub>, 500 MHz): δ 8.05 (d, *J* = 6.0 Hz, 1H, pyrimidine-H), 7.87 (s, 1H, triazole-H), 7.56 (d, *J* = 9.0 Hz, 2H, -C<sub>6</sub>H<sub>4</sub>), 7.18 (dd, *J* = 8.0, 1.5 Hz, 1H, -C<sub>6</sub>H<sub>3</sub>), 7.13 (t, *J* = 8.0 Hz, 1H, -C<sub>6</sub>H<sub>3</sub>), 6.97 (d, *J* = 9.0 Hz, 2H, -C<sub>6</sub>H<sub>4</sub>), 6.88 (dd, *J* = 8.0, 1.5 Hz, 1H, pyrimidine-H), 6.24 (d, *J* = 6.0 Hz, 1H, -C<sub>6</sub>H<sub>3</sub>), 4.49 (s, 2H, -CH<sub>2</sub>-), 3.83 (s, 3H, -OCH<sub>3</sub>), 3.79 (s, 4H, piperazine-H), 3.04 (t, *J* = 5.0 Hz, 4H, piperazine-H); <sup>13</sup>C NMR (CDCl<sub>3</sub>, 126 MHz): δ 169.9, 161.2, 159.8, 156.1, 150.7, 146.7, 134.3, 130.6, 127.8, 127.7, 125.3, 122.1, 120.7, 118.8, 114.8, 99.1 (Ar-C), 55.7 (-OCH<sub>3</sub>), 51.1, 44.1 (piperazine-C), 25.8 (-CH<sub>2</sub>-).

### 3.8. 2-(((1-(3,4-Dichlorophenyl)-1H-1,2,3-triazol-4-yl)methyl)thio)-4-(4-(2,3-dichlorophenyl)piperazin-1-yl) pyrimidine (5b)

Light yellow solid; 44% yield; mp: 172–174 °C; <sup>1</sup>H NMR (CDCl<sub>3</sub>, 500 MHz): δ 8.08 (d, *J* = 6.0 Hz, 1H, pyrimidine-H), 7.97 (s, 1H, triazole-H), 7.91–7.81 (m, 1H, -C<sub>6</sub>H<sub>3</sub>-triazole), 7.58 (d, *J* = 1.0 Hz, 2H, -C<sub>6</sub>H<sub>3</sub>-triazole), 7.21 (dd, *J* = 8.0, 1.5 Hz, 1H, -C<sub>6</sub>H<sub>3</sub>-piperazine),

7.16 (t,  $J = 8.0$  Hz, 1H,  $-C_6H_3$ -piperazine), 6.91 (dd,  $J = 8.0, 1.5$  Hz, 1H, pyrimidine-H), 6.27 (d,  $J = 6.0$  Hz, 1H,  $-C_6H_3$ -piperazine), 4.50 (s, 2H,  $-CH_2-$ ), 3.81 (s, 4H, piperazine-H), 3.06 (t,  $J = 5.0$  Hz, 4H, piperazine-H);  $^{13}C$  NMR ( $CDCl_3$ , 126 MHz):  $\delta$  169.5, 161.1, 156.0, 150.5, 147.6, 136.0, 134.1, 133.8, 132.6, 131.4, 127.6, 127.5, 125.2, 122.0, 120.2, 119.2, 118.6, 99.0 (Ar-C), 50.9, 44.0 (piperazine-C), 25.5 ( $-CH_2-$ ).

3.9. 4-(4-(((4-(4-(2,3-Dichlorophenyl) piperazin-1-yl) pyrimidin-2-yl)thio)methyl)-1H-1,2,3-triazol-1-yl)phenol (**5c**)

Brown solid; 48% yield;  $^1H$  NMR (DMSO, 500 MHz): 9.40 (s, 1H,  $-OH-C_6H_4$ ), 8.27 (s, 1H, triazole-H), 8.08 (d,  $J = 6.0$  Hz, 1H, pyrimidine-H), 7.57 (d,  $J = 8.5$  Hz, 2H,  $-C_6H_4$ ), 7.34–7.23 (m, 2H,  $-C_6H_3$ ), 7.18–7.06 (m, 1H,  $-C_6H_3$ ), 6.91 (d,  $J = 9.0$  Hz, 2H,  $-C_6H_4$ ), 6.55 (d,  $J = 6.0$  Hz, 1H, pyrimidine-H), 4.46 (s, 2H,  $-CH_2-$ ), 3.86–3.74 (m, 4H, piperazine-H), 3.15–3.03 (m, 4H, piperazine-H);  $^{13}C$  NMR (DMSO, 126 MHz):  $\delta$  168.5, 160.7, 157.3, 155.4, 150.4, 144.4, 132.4, 128.6, 127.9, 126.0, 124.3, 121.5, 120.7, 119.4, 115.6, 99.2 (Ar-C), 50.2, 43.4 (piperazine-C), 24.6 ( $-CH_2-$ ); LCMS (ESI):  $m/z$  calcd. for  $C_{23}H_{21}Cl_2N_7OS$ : 514.4301, found = 514.1631  $[M + H]^+$ , 516.1606  $[M + 2H]^+$ .

3.10. Tert-butyl 4-(2-(((1-(4-methoxyphenyl)-1H-1,2,3-triazol-4-yl)methyl)thio)pyrimidin-4-yl) piperazine-1-carboxylate (**5d**)

Yellow solid; 60% yield; mp: 94–96 °C;  $^1H$  NMR ( $CDCl_3$ , 500 MHz):  $\delta$  8.02 (d,  $J = 6.0$  Hz, 1H, pyrimidine-H), 7.84 (s, 1H, triazole-H), 7.55 (d,  $J = 9.0$  Hz, 2H,  $-C_6H_4$ ), 6.96 (d,  $J = 9.0$  Hz, 2H,  $-C_6H_4$ ), 6.17 (d,  $J = 6.5$  Hz, 1H, pyrimidine-H), 4.45 (s, 2H,  $-CH_2-$ ), 3.82 (s, 3H,  $-OCH_3$ ), 3.59 (s, 4H, piperazine-H), 3.45 (s, 4H, piperazine-H), 1.44 (s, 9H,  $-(CH_3)_3$ );  $^{13}C$  NMR ( $CDCl_3$ , 126 MHz):  $\delta$  169.8, 161.1, 159.8, 156.1, 154.7 ( $-COO$ ), 146.6, 130.6, 122.2, 120.6, 114.8, 99.0 (Ar-C), 80.4 ( $-C-(CH_3)_3$ ), 55.7 ( $-OCH_3$ ), 43.6 (piperazine-C), 28.5 ( $CH_3$ )<sub>3</sub>, 25.8 ( $-CH_2-$ ).

3.11. Tert-butyl 4-(2-(((1-(3,4-dichlorophenyl)-1H-1,2,3-triazol-4-yl)methyl)thio)pyrimidin-4-yl) piperazine-1-carboxylate (**5e**)

Yellow solid; 54% yield; mp: 153–155 °C;  $^1H$  NMR ( $CDCl_3$ , 500 MHz):  $\delta$  8.04 (d,  $J = 6.5$  Hz, 1H, pyrimidine-H), 7.93 (s, 1H, triazole-H), 7.84 (d,  $J = 1.0$  Hz, 1H,  $-C_6H_3$ ), 7.56 (s, 2H,  $-C_6H_3$ ), 6.19 (d,  $J = 6.0$  Hz, 1H, pyrimidine-H), 4.46 (s, 2H,  $-CH_2-$ ), 3.60 (s, 4H, piperazine-H), 3.47 (d,  $J = 4.5$  Hz, 4H, piperazine-H), 1.46 (s, 9H,  $-(CH_3)_3$ );  $^{13}C$  NMR ( $CDCl_3$ , 126 MHz):  $\delta$  169.6, 161.1, 156.1, 154.7 ( $-COO$ ), 147.7, 136.1, 134.0, 132.8, 131.5, 122.2, 120.3, 119.4, 99.1 (Ar-C), 80.5 ( $-C-(CH_3)_3$ ), 43.6 (piperazine-C), 28.5 ( $CH_3$ )<sub>3</sub>, 25.6 ( $-CH_2-$ ).

3.12. Tert-butyl 4-(2-(((1-(4-hydroxyphenyl)-1H-1,2,3-triazol-4-yl)methyl)thio)pyrimidin-4-yl) piperazine-1-carboxylate (**5f**)

Pink solid; 52% yield; mp: 96–98 °C;  $^1H$  NMR ( $CDCl_3$ , 500 MHz):  $\delta$  7.84 (d,  $J = 6.5$  Hz, 1H, pyrimidine-H), 7.64 (s, 1H, OH,  $-OH-C_6H_4$ ), 7.29 (d,  $J = 9.0$  Hz, 2H,  $-C_6H_4$ ), 7.07 (s, 1H, triazole-H), 6.76 (d,  $J = 9.0$  Hz, 2H,  $-C_6H_4$ ), 6.01 (d,  $J = 6.0$  Hz, 1H, pyrimidine-H), 4.28 (s, 2H,  $-CH_2-$ ), 3.44 (s, 4H, piperazine-H), 3.36–3.24 (m, 4H, piperazine-H), 1.28 (s, 9H,  $-(CH_3)_3$ );  $^{13}C$  NMR ( $CDCl_3$ , 126 MHz):  $\delta$  169.2, 160.7, 156.9, 155.4, 154.5 ( $-COO$ ), 146.3, 129.7, 122.0, 120.4, 116.2, 98.8 (Ar-C), 80.3 ( $-C-(CH_3)_3$ ), 43.4 (piperazine-C), 28.2 ( $CH_3$ )<sub>3</sub>, 25.4 ( $-CH_2-$ ).

3.13. 4-(2-(((1-(4-Methoxyphenyl)-1H-1,2,3-triazol-4-yl)methyl)thio)pyrimidin-4-yl)morpholine (**5g**)

Yellow solid; 60% yield; mp: 140–142 °C;  $^1H$  NMR ( $CDCl_3$ , 500 MHz):  $\delta$  8.10–7.97 (m, 1H, pyrimidine-H), 7.85 (s, 1H, triazole-H), 7.62–7.50 (m, 2H,  $-C_6H_4$ ), 6.97 (d,  $J = 8.5$  Hz, 2H,  $-C_6H_4$ ), 6.17 (d,  $J = 6.0$  Hz, 1H, pyrimidine-H), 4.47 (s, 2H,  $-CH_2-$ ), 3.84 (d,  $J = 0.5$  Hz, 3H,  $-OCH_3$ ), 3.78–3.66 (m, 4H, morpholine-H), 3.58 (s, 4H, morpholine-H);  $^{13}C$  NMR ( $CDCl_3$ , 126 MHz):  $\delta$  169.9, 161.3, 159.8, 156.1, 146.7, 130.6, 122.2, 120.6, 114.8, 98.9 (Ar-C), 66.5 (morpholine-C), 55.7 ( $-OCH_3$ ), 44.1 (morpholine-C), 25.8 ( $-CH_2-$ ).

3.14. 4-(2-(((1-(3,4-Dichlorophenyl)-1H-1,2,3-triazol-4-yl)methyl)thio)pyrimidin-4-yl)morpholine (**5h**)

Off-white solid; 58% yield; mp: 158–160 °C; <sup>1</sup>H NMR (CDCl<sub>3</sub>, 500 MHz): δ 7.80 (d, *J* = 6.5 Hz, 1H, pyrimidine-H), 7.68 (s, 1H, triazole-H), 7.64–7.53 (m, 1H, -C<sub>6</sub>H<sub>3</sub>), 7.36–7.26 (m, 1H, -C<sub>6</sub>H<sub>3</sub>), 7.00 (s, 1H, -C<sub>6</sub>H<sub>3</sub>), 5.93 (d, *J* = 6.5 Hz, 1H), pyrimidine-H, 4.21 (d, *J* = 0.5 Hz, 2H, -CH<sub>2</sub>-), 3.53–3.42 (m, 4H, morpholine-H), 3.33 (s, 4H, morpholine-H); <sup>13</sup>C NMR (CDCl<sub>3</sub>, 126 MHz): δ 169.5, 161.2, 155.9, 147.5, 136.0, 133.8, 132.6, 131.3, 122.0, 120.1, 119.2, 98.8 (Ar-C), 66.3, 43.9 (morpholine-C), 25.4 (-CH<sub>2</sub>-).

3.15. 4-(4-(((4-Morpholinopyrimidin-2-yl)thio)methyl)-1H-1,2,3-triazol-1-yl) phenol (**5i**)

Brown solid; 55% yield; mp: 216–218 °C; <sup>1</sup>H NMR (DMSO, 500 MHz): δ 9.89 (s, 1H, pyrimidine-H), 8.44 (s, 1H, triazole-H), 7.59 (d, *J* = 9.0 Hz, 2H, -C<sub>6</sub>H<sub>4</sub>), 6.86 (d, *J* = 9.0 Hz, 2H, -C<sub>6</sub>H<sub>4</sub>), 6.53 (d, *J* = 6.0 Hz, 1H, pyrimidine-H), 4.37 (s, 2H, -CH<sub>2</sub>-), 3.65–3.54 (m, 4H, morpholine-H), 3.55 (d, *J* = 2.5 Hz, 4H, morpholine-H); <sup>13</sup>C NMR (DMSO, 126 MHz): δ 169.2, 161.5, 158.2, 156.3, 145.4, 129.3, 122.4, 121.7, 116.5, 100.1 (Ar-C), 66.3, 44.2 (morpholine-C), 25.4 (-CH<sub>2</sub>-).

3.16. 1-(2-(((1-(4-Methoxyphenyl)-1H-1,2,3-triazol-4-yl)methyl)thio)pyrimidin-4-yl)piperidin-4-one (**5j**)

Brown solid; 58% yield; mp: 99–101 °C; <sup>1</sup>H NMR (DMSO, 400 MHz): δ 8.58 (s, 1H, triazole-H), 8.11 (d, *J* = 6.0 Hz, 1H, pyrimidine-H), 7.78 (d, *J* = 8.8 Hz, 2H, -C<sub>6</sub>H<sub>4</sub>), 7.11 (d, *J* = 9.2 Hz, 2H, -C<sub>6</sub>H<sub>4</sub>), 6.66 (d, *J* = 6.0 Hz, 1H, pyrimidine-H), 4.46 (s, 2H, -CH<sub>2</sub>-), 3.92 (s, 4H, piperidone-H), 3.82 (s, 3H, -OCH<sub>3</sub>), 2.50–2.37 (m, 4H, piperidone-H); <sup>13</sup>C NMR (DMSO, 101 MHz): δ 207.9 (-CO), 169.2, 160.9, 159.6, 156.4, 145.6, 130.5, 122.1, 121.7, 115.3, 100.0 (Ar-C), 56.0 (-OCH<sub>3</sub>), 42.3 (piperidone-C), 25.4 (-CH<sub>2</sub>-).

3.17. 1-(2-(((1-(3,4-Dichlorophenyl)-1H-1,2,3-triazol-4-yl)methyl)thio)pyrimidin-4-yl)piperidin-4-one (**5k**)

Yellow solid; 56% yield; mp: 148–150 °C; <sup>1</sup>H NMR (DMSO, 400 MHz): δ 8.80 (s, 1H, triazole-H), 8.25 (d, *J* = 2.0 Hz, 1H, -C<sub>6</sub>H<sub>3</sub>), 8.11 (d, *J* = 6.0 Hz, 1H, pyrimidine-H), 7.95 (dd, *J* = 8.8, 2.4 Hz, 1H, -C<sub>6</sub>H<sub>3</sub>), 7.84 (d, *J* = 8.8 Hz, 1H, -C<sub>6</sub>H<sub>3</sub>), 6.66 (d, *J* = 6.0 Hz, 1H, pyrimidine-H), 4.47 (s, 2H, -CH<sub>2</sub>-), 3.91 (s, 4H, piperidone-H), 2.43 (t, *J* = 6.0 Hz, 4H, piperidone-H); <sup>13</sup>C NMR (DMSO, 101 MHz): δ 207.8 (-CO), 169.1, 160.9, 156.4, 146.5, 136.6, 132.8, 132.2, 131.3, 122.1, 122.0, 120.4, 100.1 (Ar-C), 42.3 (piperidone-C), 25.2 (-CH<sub>2</sub>-).

3.18. 1-(2-(((1-(4-Hydroxyphenyl)-1H-1,2,3-triazol-4-yl)methyl)thio)pyrimidin-4-yl)piperidin-4-one (**5l**)

Yellow solid; 55% yield; <sup>1</sup>H NMR (DMSO, 400 MHz): δ 9.96 (s, 1H, -OH-C<sub>6</sub>H<sub>4</sub>), 8.49 (s, 1H, triazole-H), 8.11 (d, *J* = 6.0 Hz, 1H, pyrimidine-H), 7.63 (d, *J* = 8.8 Hz, 2H, -C<sub>6</sub>H<sub>4</sub>), 6.91 (d, *J* = 8.8 Hz, 2H, -C<sub>6</sub>H<sub>4</sub>), 6.66 (d, *J* = 6.0 Hz, 1H, pyrimidine-H), 4.44 (s, 2H, -CH<sub>2</sub>-), 3.92 (s, 4H, piperidone-H), 2.44 (t, *J* = 6.0 Hz, 4H, piperidone-H); <sup>13</sup>C NMR (DMSO, 101 MHz): δ 207.9 (-CO), 169.3, 160.9, 158.1, 156.4, 145.4, 129.2, 122.3, 121.6, 116.5, 100.1 (Ar-C), 42.3 (piperidone-C), 25.4 (-CH<sub>2</sub>-).

3.19. 5-(((4-(2,3-Dichlorophenyl) piperazin-1-yl) pyrimidin-2-yl)thio)methyl)-3-(4-methoxyphenyl) isoxazole (**6a**)

Yellow solid; 48% yield; mp: 134–136 °C; <sup>1</sup>H NMR (CDCl<sub>3</sub>, 500 MHz): δ 8.04 (d, *J* = 6.5 Hz, 1H, pyrimidine-H), 7.68 (d, *J* = 9.0 Hz, 2H, -C<sub>6</sub>H<sub>4</sub>), 7.17 (dd, *J* = 8.0, 1.0 Hz, 1H, -C<sub>6</sub>H<sub>3</sub>), 7.10 (t, *J* = 8.0 Hz, 1H, -C<sub>6</sub>H<sub>3</sub>), 6.92 (d, *J* = 9.0 Hz, 2H, -C<sub>6</sub>H<sub>4</sub>), 6.83 (dd, *J* = 8.0, 1.0 Hz, 1H, -C<sub>6</sub>H<sub>3</sub>), 6.49 (s, 1H, isoxazole-H), 6.24 (d, *J* = 6.0 Hz, 1H, pyrimidine-H), 4.39 (s, 2H, -CH<sub>2</sub>-), 3.82 (s, 3H, -OCH<sub>3</sub>), 3.77 (s, 4H, piperazine-H), 3.08–2.96 (m, 4H, piperazine-H); <sup>13</sup>C NMR (CDCl<sub>3</sub>, 126 MHz): δ 170.9, 168.9, 162.2, 161.2, 161.0, 156.1, 150.6, 134.2, 128.2, 127.8, 127.6, 125.3, 121.7, 118.8, 114.3, 100.2, 99.3 (Ar-C), 55.4 (-OCH<sub>3</sub>), 51.0, 44.2 (piperazine-C), 26.0 (-CH<sub>2</sub>-); LCMS (ESI): *m/z* calcd. for C<sub>25</sub>H<sub>23</sub>Cl<sub>2</sub>N<sub>5</sub>O<sub>2</sub>S: 528.4534, found = 528.2081 [M + H]<sup>+</sup>, 530.2043 [M + 2H]<sup>+</sup>.

3.20. 5-(((4-(2,3-Dichlorophenyl) piperazin-1-yl) pyrimidin-2-yl)thio)methyl)-3-(3,4-dimethoxyphenyl)isoxazole (**6b**)

Yellow solid; 40% yield; mp: 126–128 °C; <sup>1</sup>H NMR (CDCl<sub>3</sub>, 500 MHz): δ 8.04 (d, *J* = 6.0 Hz, 1H, pyrimidine-H), 7.36 (d, *J* = 1.5 Hz, 1H, -C<sub>6</sub>H<sub>3</sub>-isoxazole), 7.17 (d, *J* = 8.0 Hz, 1H, -C<sub>6</sub>H<sub>3</sub>-isoxazole), 7.09 (t, *J* = 8.0 Hz, 1H, -C<sub>6</sub>H<sub>3</sub>-piperazine), 6.95–6.82 (m, 2H, -C<sub>6</sub>H<sub>3</sub>-piperazine), 6.82 (d, *J* = 8.0 Hz, 1H, -C<sub>6</sub>H<sub>3</sub>-isoxazole), 6.51 (s, 1H, isoxazole-H), 6.24 (d, *J* = 6.5 Hz, 1H, pyrimidine-H), 4.39 (s, 2H, -CH<sub>2</sub>-), 3.90 (s, 6H, (OCH<sub>3</sub>)<sub>2</sub>), 3.77 (s, 4H, piperazine-H), 3.02 (t, *J* = 4.5 Hz, 4H, piperazine-H); <sup>13</sup>C NMR (CDCl<sub>3</sub>, 126 MHz): δ 171.0, 168.9, 162.3, 161.2, 156.1, 150.6, 149.3, 134.3, 127.6, 125.3, 121.8, 120.0, 118.7, 113.5, 112.5, 111.0, 109.2, 100.3, 99.3 (Ar-C), 56.1, 56.0 (-OCH<sub>3</sub>), 51.0, 44.2 (piperazine-C), 26.0(-CH<sub>2</sub>-); LCMS (ESI): *m/z* calcd. for C<sub>26</sub>H<sub>25</sub>Cl<sub>2</sub>N<sub>5</sub>O<sub>3</sub>S: 558.4794, found = 558.2141 [M + H]<sup>+</sup>, 560.2081 [M + 2H]<sup>+</sup>.

3.21. 5-(((4-(2,3-Dichlorophenyl) piperazin-1-yl) pyrimidin-2-yl)thio)methyl)-3-(*p*-tolyl)isoxazole (**6c**)

Yellow solid; 52% yield; mp: 98–100 °C; <sup>1</sup>H NMR (CDCl<sub>3</sub>, 500 MHz): δ 7.78 (d, *J* = 6.0 Hz, 1H, pyrimidine-H), 7.38 (d, *J* = 8.0 Hz, 2H, -C<sub>6</sub>H<sub>4</sub>), 6.95 (d, *J* = 7.5 Hz, 2H, -C<sub>6</sub>H<sub>4</sub>), 6.97–6.86 (m, 1H, -C<sub>6</sub>H<sub>3</sub>), 6.84 (t, *J* = 8.0 Hz, 1H, -C<sub>6</sub>H<sub>3</sub>), 6.57 (dd, *J* = 8.0, 1.5 Hz, 1H, -C<sub>6</sub>H<sub>3</sub>), 6.26 (s, 1H, isoxazole-H), 5.98 (d, *J* = 6.0 Hz, 1H, pyrimidine-H), 4.14 (s, 2H, -CH<sub>2</sub>-), 3.51 (s, 4H, piperazine-H), 2.76 (t, *J* = 5.0 Hz, 4H, piperazine-H), 2.10 (s, 3H, -CH<sub>3</sub>); <sup>13</sup>C NMR (CDCl<sub>3</sub>, 126 MHz): δ 170.7, 168.6, 162.3, 160.9, 155.9, 150.4, 139.9, 134.0, 129.4, 127.5, 127.3, 126.4, 126.0, 125.0, 118.5, 100.1, 99.0 (Ar-C), 50.7, 43.9 (piperazine-C), 25.7 (-CH<sub>2</sub>-), 21.2 (-CH<sub>3</sub>).

3.22. *Tert*-butyl 4-(2-(((3-(4-methoxyphenyl) isoxazol-5-yl)methyl)thio)pyrimidin-4-yl)piperazine-1-carboxylate (**6d**)

Yellow solid; 55% yield; mp: 120–122 °C; <sup>1</sup>H NMR (CDCl<sub>3</sub>, 500 MHz): δ 8.03 (d, *J* = 6.5 Hz, 1H, pyrimidine-H), 7.68 (d, *J* = 8.5 Hz, 2H, -C<sub>6</sub>H<sub>4</sub>), 6.93 (d, *J* = 8.5 Hz, 2H, -C<sub>6</sub>H<sub>4</sub>), 6.47 (s, 1H, isoxazole-H), 6.19 (d, *J* = 6.5 Hz, 1H, pyrimidine-H), 4.38 (s, 2H, -CH<sub>2</sub>-), 3.82 (s, 3H, -OCH<sub>3</sub>), 3.59 (s, 4H, piperazine-H), 3.47 (s, 4H, piperazine-H), 1.46 (s, 9H, -(CH<sub>3</sub>)<sub>3</sub>); <sup>13</sup>C NMR (CDCl<sub>3</sub>, 126 MHz): δ 170.9, 168.9, 162.2, 161.1, 161.0, 156.2, 154.7 (-COO), 128.2, 121.7, 114.3, 100.3, 99.2 (Ar-C), 80.4 (-C-(CH<sub>3</sub>)<sub>3</sub>), 55.4 (-OCH<sub>3</sub>), 43.6 (piperazine-C), 28.5 (CH<sub>3</sub>)<sub>3</sub>, 25.9 (-CH<sub>2</sub>-); LCMS (ESI): *m/z* calcd. for C<sub>24</sub>H<sub>29</sub>N<sub>5</sub>O<sub>4</sub>S: 483.5832, found = 484.1700 [M + H]<sup>+</sup>.

3.23. *Tert*-butyl 4-(2-(((3-(3,4-dimethoxyphenyl) isoxazol-5-yl)methyl)thio)pyrimidin-4-yl)piperazine-1-carboxylate (**6e**)

Brown solid; 52% yield; mp: 85–87 °C; <sup>1</sup>H NMR (DMSO, 400 MHz): δ 8.07 (d, *J* = 6.4 Hz, 1H, pyrimidine-H), 7.46–7.32 (m, 2H, -C<sub>6</sub>H<sub>3</sub>), 7.04 (d, *J* = 8.4 Hz, 1H, -C<sub>6</sub>H<sub>3</sub>), 6.92 (s, 1H, isoxazole-H), 6.58 (d, *J* = 6.0 Hz, 1H, pyrimidine-H), 4.51 (s, 2H, -CH<sub>2</sub>-), 3.82 (s, 3H, -OCH<sub>3</sub>), 3.80 (s, 3H, -OCH<sub>3</sub>), 3.61 (s, 4H, piperazine-H), 3.44–3.32 (s, 4H, piperazine-H), 1.41 (s, 9H, -(CH<sub>3</sub>)<sub>3</sub>); <sup>13</sup>C NMR (DMSO, 101 MHz): δ 171.1, 168.3, 162.3, 161.2, 156.4, 154.3, 150.8, 149.5, 121.5, 120.0, 112.3, 110.0, 100.9, 100.3 (Ar-C), 79.6 (-C-(CH<sub>3</sub>)<sub>3</sub>), 56.0, 56.0 (-OCH<sub>3</sub>), 43.5 (piperazine-C), 28.5 (CH<sub>3</sub>)<sub>3</sub>, 25.5 (-CH<sub>2</sub>-); LCMS (ESI): *m/z* calcd. for C<sub>25</sub>H<sub>31</sub>N<sub>5</sub>O<sub>5</sub>S: 513.6091, found = 514.2142 [M + H]<sup>+</sup>.

3.24. *Tert*-butyl 4-(2-(((3-(*p*-tolyl) isoxazol-5-yl)methyl)thio)pyrimidin-4-yl)piperazine-1-carboxylate (**6f**)

Off-white solid; 60% yield; mp: 141–143 °C; <sup>1</sup>H NMR (CDCl<sub>3</sub>, 500 MHz): δ 7.83 (d, *J* = 6.5 Hz, 1H, pyrimidine-H), 7.43 (d, *J* = 8.0 Hz, 2H, -C<sub>6</sub>H<sub>4</sub>), 7.01 (d, *J* = 8.0 Hz, 2H, -C<sub>6</sub>H<sub>4</sub>), 6.30 (s, 1H, isoxazole-H), 5.99 (d, *J* = 6.5 Hz, 1H, pyrimidine-H), 4.19 (s, 2H, -CH<sub>2</sub>-), 3.39 (s, 4H, piperazine-H), 3.27 (s, 4H, piperazine-H), 2.16 (s, 3H, -CH<sub>3</sub>), 1.26 (s, 9H, -(CH<sub>3</sub>)<sub>3</sub>); <sup>13</sup>C NMR (CDCl<sub>3</sub>, 126 MHz): δ 170.7, 168.7, 162.4, 160.9, 156.0, 154.5 (-COO), 140.0, 129.4, 126.5, 126.1, 100.2, 99.0 (Ar-C), 80.2 (-C-(CH<sub>3</sub>)<sub>3</sub>), 43.4 (piperazine-C), 28.3 (CH<sub>3</sub>)<sub>3</sub>, 25.7 (-CH<sub>2</sub>-), 21.3 (-CH<sub>3</sub>).



**3.25. 4-(2-(((3-(4-Methoxyphenyl) isoxazol-5-yl)methyl)thio) pyrimidin-4-yl)morpholine (6g)**

Yellow solid; 54% yield; mp: 104–106 °C; <sup>1</sup>H NMR (CDCl<sub>3</sub>, 500 MHz): δ 8.03 (d, *J* = 6.5 Hz, 1H, pyrimidine-H), 7.68 (d, *J* = 9.0 Hz, 2H, -C<sub>6</sub>H<sub>4</sub>), 6.93 (d, *J* = 9.0 Hz, 2H, -C<sub>6</sub>H<sub>4</sub>), 6.47 (s, 1H, isoxazole-H), 6.17 (d, *J* = 6.0 Hz, 1H, pyrimidine-H), 4.38 (s, 2H, -CH<sub>2</sub>-), 3.82 (s, 3H, -OCH<sub>3</sub>), 3.78–3.66 (m, 4H, morpholine-H), 3.57 (s, 4H, morpholine-H); <sup>13</sup>C NMR (CDCl<sub>3</sub>, 126 MHz): δ 170.8, 168.9, 162.2, 161.3, 161.0, 156.1, 128.2, 121.7, 114.3, 100.3, 99.1 (Ar-C), 66.5 (morpholine-C), 55.4 (-OCH<sub>3</sub>), 44.1 (morpholine-C), 25.9 (-CH<sub>2</sub>-); LCMS (ESI): *m/z* calcd. for C<sub>19</sub>H<sub>20</sub>N<sub>4</sub>O<sub>3</sub>S: 384.4521, found = 385.1061 [M + H]<sup>+</sup>.

**3.26. 4-(2-(((3-(3,4-Dimethoxyphenyl) isoxazol-5-yl)methyl)thio) pyrimidin-4-yl)morpholine (6h)**

Yellow solid; 48% yield; mp: 118–120 °C; <sup>1</sup>H NMR (CDCl<sub>3</sub>, 500 MHz): δ 8.03 (d, *J* = 6.0 Hz, 1H, pyrimidine-H), 7.35 (d, *J* = 1.0 Hz, 1H, -C<sub>6</sub>H<sub>3</sub>), 7.23 (dd, *J* = 8.5, 1.0 Hz, 1H, -C<sub>6</sub>H<sub>3</sub>), 6.88 (d, *J* = 8.5 Hz, 1H, -C<sub>6</sub>H<sub>3</sub>), 6.49 (s, 1H, isoxazole-H), 6.18 (d, *J* = 6.0 Hz, 1H, pyrimidine-H), 4.38 (s, 2H, -CH<sub>2</sub>-), 3.91 (s, 3H, -OCH<sub>3</sub>), 3.89 (s, 3H, -OCH<sub>3</sub>), 3.78–3.66 (m, 4H, morpholine-H), 3.57 (s, 4H, morpholine-H); <sup>13</sup>C NMR (CDCl<sub>3</sub>, 126 MHz): δ 171.0, 168.9, 162.3, 161.4, 156.1, 150.6, 149.3, 121.8, 119.9, 111.1, 109.3, 100.3, 99.1 (Ar-C), 66.5 (morpholine-C), 56.1, 56.0 (-OCH<sub>3</sub>), 44.1 (morpholine-C), 25.9 (-CH<sub>2</sub>-); LCMS (ESI): *m/z* calcd. for C<sub>20</sub>H<sub>22</sub>N<sub>4</sub>O<sub>4</sub>S: 414.4781, found = 415.1629 [M + H]<sup>+</sup>.

**3.27. 4-(2-(((3-(*p*-tolyl) isoxazol-5-yl)methyl)thio) pyrimidin-4-yl)morpholine (6i)**

Off-white solid; 58% yield; mp: 128–130 °C; <sup>1</sup>H NMR (CDCl<sub>3</sub>, 500 MHz): δ 8.04 (d, *J* = 6.0 Hz, 1H, pyrimidine-H), 7.63 (d, *J* = 8.0 Hz, 2H, -C<sub>6</sub>H<sub>4</sub>), 7.22 (d, *J* = 8.0 Hz, 2H, -C<sub>6</sub>H<sub>4</sub>), 6.50 (s, 1H, isoxazole-H), 6.18 (d, *J* = 6.0 Hz, 1H, pyrimidine-H), 4.39 (s, 2H, -CH<sub>2</sub>-), 3.78–3.66 (m, 4H, morpholine-H), 3.57 (s, 4H, morpholine-H), 2.37 (s, 3H, -CH<sub>3</sub>); <sup>13</sup>C NMR (CDCl<sub>3</sub>, 126 MHz): δ 170.9, 168.9, 162.6, 161.3, 156.1, 140.2, 129.6, 126.7, 126.3, 100.4, 99.1 (Ar-C), 66.5, 44.1 (morpholine-C), 25.9 (-CH<sub>2</sub>-), 21.5 (-CH<sub>3</sub>).

**3.28. 1-(2-(((3-(4-methoxyphenyl) isoxazol-5-yl)methyl)thio) pyrimidin-4-yl) piperidin-4-one (6j)**

Yellow solid; 50% yield; mp: 125–127 °C; <sup>1</sup>H NMR (DMSO, 400 MHz): δ 8.11 (d, *J* = 6.4 Hz, 1H, pyrimidine-H), 7.78 (d, *J* = 8.8 Hz, 2H, -C<sub>6</sub>H<sub>4</sub>), 7.03 (d, *J* = 8.8 Hz, 2H, -C<sub>6</sub>H<sub>4</sub>), 6.87 (s, 1H, isoxazole-H), 6.68 (d, *J* = 6.4 Hz, 1H, pyrimidine-H), 4.53 (s, 2H, -CH<sub>2</sub>-), 3.91 (s, 4H, piperidone-H), 3.81 (s, 3H, -OCH<sub>3</sub>), 2.49–2.36 (m, 4H, piperidone-H); <sup>13</sup>C NMR (DMSO, 101 MHz): δ 207.8 (-CO), 171.2, 168.3, 162.0, 161.1, 160.9, 156.5, 128.5, 121.4, 114.9, 100.7, 100.3 (Ar-C), 55.7 (-OCH<sub>3</sub>), 42.2 (piperidone-C), 25.4 (-CH<sub>2</sub>-).

**3.29. 1-(2-(((3-(3,4-dimethoxyphenyl) isoxazol-5-yl)methyl)thio) pyrimidin-4-yl) piperidin-4-one (6k)**

Yellow solid; 44% yield; mp: 104–106 °C; <sup>1</sup>H NMR (DMSO, 400 MHz): δ 8.11 (d, *J* = 6.0 Hz, 1H, pyrimidine-H), 7.39 (d, *J* = 8.4 Hz, 2H, -C<sub>6</sub>H<sub>3</sub>), 7.04 (d, *J* = 8.4 Hz, 1H, -C<sub>6</sub>H<sub>3</sub>), 6.92 (s, 1H, isoxazole-H), 6.67 (d, *J* = 6.4 Hz, 1H, pyrimidine-H), 4.53 (s, 2H, -CH<sub>2</sub>-), 3.91 (s, 4H, piperidone-H), 3.82 (s, 3H, -OCH<sub>3</sub>), 3.80 (s, 3H, -OCH<sub>3</sub>), 2.43 (t, *J* = 6.0 Hz, 4H, piperidone-H); <sup>13</sup>C NMR (DMSO, 101 MHz): δ 207.8 (-CO), 171.2, 168.4, 162.3, 160.9, 156.5, 150.8, 149.5, 121.5, 120.0, 112.3, 110.0, 100.9, 100.3 (Ar-C), 56.1, 56.0 (-OCH<sub>3</sub>), 42.2 (piperidone-C), 25.5 (-CH<sub>2</sub>-); LCMS (ESI): *m/z* calcd. for C<sub>21</sub>H<sub>22</sub>N<sub>4</sub>O<sub>4</sub>S: 426.4888, found = 427.2091 [M + H]<sup>+</sup>.

**3.30. 1-(2-(((3-(*p*-tolyl) isoxazol-5-yl)methyl)thio) pyrimidin-4-yl) piperidin-4-one (6l)**

Light yellow solid; 56% yield; mp: 122–124 °C; <sup>1</sup>H NMR (DMSO, 400 MHz): δ 8.11 (d, *J* = 6.0 Hz, 1H, pyrimidine-H), 7.73 (d, *J* = 8.0 Hz, 2H, -C<sub>6</sub>H<sub>4</sub>), 7.30 (d, *J* = 8.0 Hz, 2H, -C<sub>6</sub>H<sub>4</sub>), 6.89 (s, 1H, isoxazole-H), 6.68 (d, *J* = 6.0 Hz, 1H, pyrimidine-H), 4.54 (s, 2H, -CH<sub>2</sub>-), 3.91 (s, 4H, piperidone-H), 2.43 (t, *J* = 6.0 Hz, 4H, piperidone-H), 2.35 (s, 3H, -CH<sub>3</sub>); <sup>13</sup>C NMR (DMSO, 101 MHz): δ 207.8 (-CO), 171.4, 168.3, 162.3, 160.9, 156.5, 140.4, 130.1, 126.9, 126.2, 100.9, 100.3 (Ar-C), 42.2 (piperidone-C), 25.4 (-CH<sub>2</sub>-), 21.4 (-CH<sub>3</sub>).

3.31. 2-(((1-(4-Methoxyphenyl)-1H-1,2,3-triazol-4-yl)methyl)thio)-4-(piperazin-1-yl)pyrimidine (**7a**)

Thick brown mass; 70% yield;  $^1\text{H}$  NMR ( $\text{CDCl}_3$ , 500 MHz):  $\delta$  8.00 (d,  $J = 6.0$  Hz, 1H, pyrimidine-H), 7.84 (s, 1H, triazole-H), 7.60–7.49 (m, 2H,  $-\text{C}_6\text{H}_4$ ), 7.02–6.90 (m, 2H,  $-\text{C}_6\text{H}_4$ ), 6.16 (d,  $J = 6.5$  Hz, 1H, pyrimidine-H), 4.45 (s, 2H,  $-\text{CH}_2-$ ), 3.82 (s, 3H,  $-\text{OCH}_3$ ), 3.59 (s, 4H, piperazine-H), 2.95–2.83 (m, 4H, piperazine-H);  $^{13}\text{C}$  NMR ( $\text{CDCl}_3$ , 126 MHz):  $\delta$  169.7, 161.1, 159.8, 155.9, 146.7, 130.6, 122.2, 120.7, 114.8, 98.9 (Ar-C), 55.7 ( $-\text{OCH}_3$ ), 45.5, 44.6 (piperazine-C), 25.7 ( $-\text{CH}_2-$ ).

3.32. 2-(((1-(3,4-Dichlorophenyl)-1H-1,2,3-triazol-4-yl)methyl)thio)-4-(piperazin-1-yl)pyrimidine (**7b**)

Thick brown mass; 50% yield;  $^1\text{H}$  NMR ( $\text{CDCl}_3$ , 500 MHz):  $\delta$  7.79 (d,  $J = 6.0$  Hz, 1H, pyrimidine-H), 7.71 (s, 1H, triazole-H), 7.67–7.57 (m, 1H,  $-\text{C}_6\text{H}_3$ ), 7.33 (d,  $J = 1.0$  Hz, 2H,  $-\text{C}_6\text{H}_3$ ), 5.96 (d,  $J = 6.0$  Hz, 1H, pyrimidine-H), 4.24 (s, 2H,  $-\text{CH}_2-$ ), 3.37 (s, 4H, piperazine-H), 2.73–2.61 (m, 4H, piperazine-H);  $^{13}\text{C}$  NMR ( $\text{CDCl}_3$ , 126 MHz):  $\delta$  169.3, 161.0, 155.7, 147.5, 135.9, 133.8, 132.5, 131.3, 122.0, 120.1, 119.2, 98.8 (Ar-C), 45.5, 44.6 (piperazine-C), 25.4 ( $-\text{CH}_2-$ ).

3.33. 4-(4-(((4-(Piperazin-1-yl)pyrimidin-2-yl)thio)methyl)-1H-1,2,3-triazol-1-yl)phenol (**7c**)

Yellow solid; 58% yield; mp: 204–206 °C;  $^1\text{H}$  NMR (DMSO, 500 MHz):  $\delta$  8.41 (s, 1H, triazole-H), 7.97 (d,  $J = 6.0$  Hz, 1H, pyrimidine-H), 7.56 (d,  $J = 8.5$  Hz, 2H,  $-\text{C}_6\text{H}_4$ ), 6.87 (d,  $J = 9.0$  Hz, 2H,  $-\text{C}_6\text{H}_4$ ), 6.48 (d,  $J = 6.0$  Hz, 1H, pyrimidine-H), 4.35 (s, 2H,  $-\text{CH}_2-$ ), 3.47 (s, 4H, piperazine-H), 2.65 (s, 4H, piperazine-H);  $^{13}\text{C}$  NMR (DMSO, 126 MHz):  $\delta$  169.1, 161.2, 158.8, 156.1, 145.4, 128.9, 122.3, 121.7, 116.6, 99.9 (Ar-C), 45.8, 45.2 (piperazine-C), 25.3 ( $-\text{CH}_2-$ ).

3.34. 3-(4-Methoxyphenyl)-5-(((4-(piperazin-1-yl)pyrimidin-2-yl)thio)methyl)isoxazole (**7d**)

Yellow solid; 60% yield; mp: 88–90 °C;  $^1\text{H}$  NMR ( $\text{CDCl}_3$ , 500 MHz):  $\delta$  8.02 (d,  $J = 4.5$  Hz, 1H, pyrimidine-H), 7.70 (d,  $J = 7.5$  Hz, 2H,  $-\text{C}_6\text{H}_4$ ), 6.94 (d,  $J = 7.5$  Hz, 2H,  $-\text{C}_6\text{H}_4$ ), 6.49 (s, 1H, isoxazole-H), 6.20 (d,  $J = 4.5$  Hz, 1H, pyrimidine-H), 4.40 (s, 2H,  $-\text{CH}_2-$ ), 3.84 (s, 3H,  $-\text{OCH}_3$ ), 3.60 (s, 4H, piperazine-H), 2.91 (s, 4H, piperazine-H);  $^{13}\text{C}$  NMR ( $\text{CDCl}_3$ , 126 MHz):  $\delta$  172.9, 170.7, 164.2, 163.1, 162.9, 157.9, 130.2, 123.6, 116.3, 102.2, 101.0 (Ar-C), 57.4 ( $-\text{OCH}_3$ ), 47.6, 46.8 (piperazine-C), 27.8 ( $-\text{CH}_2-$ ); LCMS (ESI):  $m/z$  calcd. for  $\text{C}_{19}\text{H}_{21}\text{N}_5\text{O}_2\text{S}$ : 383.4673, found = 384.2190  $[\text{M} + \text{H}]^+$ .

3.35. 3-(3,4-Dimethoxyphenyl)-5-(((4-(piperazin-1-yl)pyrimidin-2-yl)thio)methyl)isoxazole (**7e**)

Thick brown mass; 54% yield;  $^1\text{H}$  NMR ( $\text{CDCl}_3$ , 500 MHz):  $\delta$  8.02 (d,  $J = 6.5$  Hz, 1H, pyrimidine-H), 7.37 (d,  $J = 2.0$  Hz, 1H,  $-\text{C}_6\text{H}_3$ ), 7.25 (dd,  $J = 8.0, 2.0$  Hz, 1H,  $-\text{C}_6\text{H}_3$ ), 6.90 (d,  $J = 8.0$  Hz, 1H,  $-\text{C}_6\text{H}_3$ ), 6.51 (s, 1H, isoxazole-H), 6.20 (d,  $J = 6.5$  Hz, 1H, pyrimidine-H), 4.41 (s, 2H,  $-\text{CH}_2-$ ), 3.94 (s, 3H,  $-\text{OCH}_3$ ), 3.92 (s, 3H,  $-\text{OCH}_3$ ), 3.59 (s, 4H, piperazine-H), 2.90 (t,  $J = 5.0$  Hz, 4H, piperazine-H);  $^{13}\text{C}$  NMR ( $\text{CDCl}_3$ , 126 MHz):  $\delta$  171.0, 168.7, 162.3, 161.2, 155.9, 150.6, 149.3, 121.9, 119.9, 111.1, 109.3, 100.3, 99.1 (Ar-C), 56.1, 56.0 ( $-\text{OCH}_3$ ), 45.7, 44.9 (piperazine-C), 25.9 ( $-\text{CH}_2-$ ).

3.36. 5-(((4-(Piperazin-1-yl)pyrimidin-2-yl)thio)methyl)-3-(*p*-tolyl)isoxazole (**7f**)

Thick light brown mass; 64% yield;  $^1\text{H}$  NMR ( $\text{CDCl}_3$ , 500 MHz):  $\delta$  8.02 (d,  $J = 6.5$  Hz, 1H, pyrimidine-H), 7.65 (d,  $J = 8.0$  Hz, 2H,  $-\text{C}_6\text{H}_4$ ), 7.23 (d,  $J = 8.0$  Hz, 2H,  $-\text{C}_6\text{H}_4$ ), 6.52 (s, 1H, isoxazole-H), 6.19 (d,  $J = 6.0$  Hz, 1H, pyrimidine-H), 4.40 (s, 2H,  $-\text{CH}_2-$ ), 3.61 (s, 4H, piperazine-H), 2.92 (s, 4H, piperazine-H), 2.38 (s, 3H,  $-\text{CH}_3$ );  $^{13}\text{C}$  NMR ( $\text{CDCl}_3$ , 126 MHz):  $\delta$  171.0, 168.8, 162.5, 161.1, 156.0, 140.1, 129.6, 126.7, 126.3, 100.4, 99.1 (Ar-C), 45.6, 44.7 (piperazine-C), 25.9 ( $-\text{CH}_2-$ ), 21.5 ( $-\text{CH}_3$ ).

3.37. 1-(2-(((1-(4-Methoxyphenyl)-1H-1,2,3-triazol-4-yl)methyl)thio)pyrimidin-4-yl)piperidin-4-ol (**8a**)

Thick off-white mass; 60% yield;  $^1\text{H}$  NMR ( $\text{CDCl}_3$ , 500 MHz):  $\delta$  7.99 (d,  $J = 6.5$  Hz, 1H, pyrimidine-H), 7.85 (s, 1H, triazole-H), 7.56 (d,  $J = 9.0$  Hz, 2H,  $-\text{C}_6\text{H}_4$ ), 6.97 (d,  $J = 9.0$  Hz, 2H,  $-\text{C}_6\text{H}_4$ ), 6.21 (d,  $J = 6.5$  Hz, 1H, pyrimidine-H), 4.47 (s, 2H,  $-\text{CH}_2-$ ), 4.06–3.88 (m, 4H, piperidine-H (3H) and OH (1H)), 3.83 (s, 3H,  $-\text{OCH}_3$ ), 3.35–3.20 (m, 2H, piperidine-H), 1.96–1.82 (m, 2H, piperidine-H), 1.58–1.41 (m, 2H, piperidine-H);  $^{13}\text{C}$  NMR ( $\text{CDCl}_3$ , 126 MHz):  $\delta$  169.7, 160.8, 159.8, 155.9, 146.7, 130.6, 122.2, 120.7, 114.8, 98.9 (Ar-C), 67.3 (piperidine-C (quaternary)), 55.7 ( $-\text{OCH}_3$ ), 41.3, 33.7 (piperidine-C), 25.8 ( $-\text{CH}_2-$ ).

3.38. 1-(2-(((1-(3,4-Dichlorophenyl)-1H-1,2,3-triazol-4-yl)methyl)thio)pyrimidin-4-yl)piperidin-4-ol (**8b**)

Thick pink mass; 55% yield;  $^1\text{H}$  NMR ( $\text{CDCl}_3$ , 500 MHz):  $\delta$  7.97 (d,  $J = 6.5$  Hz, 1H, pyrimidine-H), 7.94 (s, 1H, triazole-H), 7.83 (t,  $J = 1.5$  Hz, 1H,  $-\text{C}_6\text{H}_3$ ), 7.54 (d,  $J = 1.5$  Hz, 2H,  $-\text{C}_6\text{H}_3$ ), 6.21 (d,  $J = 6.5$  Hz, 1H, pyrimidine-H), 4.45 (s, 2H,  $-\text{CH}_2-$ ), 4.16–3.88 (m, 4H, piperidine-H (3H) and OH (1H)), 3.34–3.19 (m, 2H, piperidine-H), 1.95–1.81 (m, 2H, piperidine-H), 1.58–1.41 (m, 2H, piperidine-H);  $^{13}\text{C}$  NMR ( $\text{CDCl}_3$ , 126 MHz):  $\delta$  169.4, 160.8, 155.8, 147.7, 136.1, 134.0, 132.8, 131.5, 122.2, 120.4, 119.4, 99.0 (Ar-C), 67.1 (piperidine-C (quaternary)), 41.4, 33.7 (piperidine-C), 25.6 ( $-\text{CH}_2-$ ); LCMS (ESI):  $m/z$  calcd. for  $\text{C}_{18}\text{H}_{18}\text{Cl}_2\text{N}_6\text{O}$ : 437.3461, found = 437.1480  $[\text{M} + \text{H}]^+$ , 439.1444  $[\text{M} + 2\text{H}]^+$ .

3.39. 1-(2-(((1-(4-Hydroxyphenyl)-1H-1,2,3-triazol-4-yl)methyl)thio)pyrimidin-4-yl)piperidin-4-ol (**8c**)

Yellow solid; 58% yield; mp: 104–106 °C;  $^1\text{H}$  NMR (DMSO, 400 MHz):  $\delta$  9.94 (s, 1H,  $-\text{OH}-\text{C}_6\text{H}_4$ ), 8.47 (s, 1H, triazole-H), 8.01 (d,  $J = 6.0$  Hz, 1H, pyrimidine-H), 7.63 (d,  $J = 8.8$  Hz, 2H,  $-\text{C}_6\text{H}_4$ ), 6.91 (d,  $J = 8.4$  Hz, 2H,  $-\text{C}_6\text{H}_4$ ), 6.57 (d,  $J = 6.0$  Hz, 1H, pyrimidine-H), 4.77 (d,  $J = 3.2$  Hz, 1H, piperidine-H), 4.41 (s, 2H,  $-\text{CH}_2-$ ), 4.01 (d,  $J = 6.8$  Hz, 2H, piperidine-H (1H) and OH (1H)), 3.74 (d,  $J = 3.2$  Hz, 1H, piperidine-H), 3.31–3.16 (m, 2H, piperidine-H), 1.75 (d,  $J = 9.2$  Hz, 2H, piperidine-H), 1.31 (d,  $J = 9.2$  Hz, 2H, piperidine-H);  $^{13}\text{C}$  NMR (DMSO, 101 MHz):  $\delta$  169.1, 160.9, 158.1, 156.1, 145.4, 129.2, 122.3, 121.6, 116.5, 99.9 (Ar-C), 66.0 (piperidine-C (quaternary)), 41.6, 34.1 (piperidine-C), 25.3 ( $-\text{CH}_2-$ ); LCMS (ESI):  $m/z$  calcd. for  $\text{C}_{18}\text{H}_{20}\text{N}_6\text{O}_2\text{S}$ : 384.4554, found = 385.1543  $[\text{M} + \text{H}]^+$ .

3.40. 1-(2-(((3-(4-Methoxyphenyl) isoxazol-5-yl)methyl)thio)pyrimidin-4-yl)piperidin-4-ol (**8d**)

Yellow solid; 64% yield; mp: 98–100 °C;  $^1\text{H}$  NMR ( $\text{CDCl}_3$ , 500 MHz):  $\delta$  7.98 (d,  $J = 6.5$  Hz, 1H, pyrimidine-H), 7.67 (d,  $J = 9.0$  Hz, 2H,  $-\text{C}_6\text{H}_4$ ), 6.92 (d,  $J = 8.5$  Hz, 2H,  $-\text{C}_6\text{H}_4$ ), 6.47 (s, 1H isoxazole-H), 6.21 (d,  $J = 6.0$  Hz, 1H, pyrimidine-H), 4.38 (s, 2H,  $-\text{CH}_2-$ ), 4.02–3.86 (m, 4H piperidine-H (3H) and OH (1H)), 3.82 (s, 3H,  $-\text{OCH}_3$ ), 3.35–3.20 (m, 2H, piperidine-H), 1.96–1.81 (m, 2H, piperidine-H), 1.58–1.41 (m, 2H, piperidine-H);  $^{13}\text{C}$  NMR ( $\text{CDCl}_3$ , 126 MHz):  $\delta$  171.0, 168.8, 162.2, 161.0, 160.8, 155.9, 128.2, 121.7, 114.3, 100.3, 99.1 (Ar-C), 67.2 (piperidine-C (quaternary)), 55.4 ( $-\text{OCH}_3$ ), 41.3, 33.7 (piperidine-C), 25.9 ( $-\text{CH}_2-$ ); LCMS (ESI):  $m/z$  calcd. for  $\text{C}_{20}\text{H}_{22}\text{N}_4\text{O}_3\text{S}$ : 398.4787, found = 399.1363  $[\text{M} + \text{H}]^+$ .

3.41. 1-(2-(((3-(3,4-Dimethoxyphenyl) isoxazol-5-yl)methyl)thio)pyrimidin-4-yl)piperidin-4-ol (**8e**)

Thick off-white mass; 58% yield;  $^1\text{H}$  NMR ( $\text{CDCl}_3$ , 500 MHz):  $\delta$  8.00 (d,  $J = 6.5$  Hz, 1H, pyrimidine-H), 7.37 (d,  $J = 1.5$  Hz, 1H,  $-\text{C}_6\text{H}_3$ ), 7.25 (dd,  $J = 8.5, 1.5$  Hz, 1H,  $-\text{C}_6\text{H}_3$ ), 6.90 (d,  $J = 8.5$  Hz, 1H,  $-\text{C}_6\text{H}_3$ ), 6.52 (s, 1H, isoxazole-H), 6.24 (d,  $J = 6.5$  Hz, 1H, pyrimidine-H), 4.41 (s, 2H,  $-\text{CH}_2-$ ), 4.07–3.91 (m, 4H, piperidine-H (3H) and OH (1H)), 3.94 (s, 3H,  $-\text{OCH}_3$ ), 3.92 (s, 3H,  $-\text{OCH}_3$ ), 3.37–3.23 (m, 2H, piperidine-H), 1.99–1.85 (m, 2H, piperidine-H), 1.61–1.44 (m, 2H, piperidine-H);  $^{13}\text{C}$  NMR ( $\text{CDCl}_3$ , 126 MHz):  $\delta$  171.1, 168.8, 162.3, 160.8, 155.9, 150.6, 149.3, 121.9, 119.9, 111.1, 109.3, 100.3, 99.1 (Ar-C), 67.2 (piperidine-C (quaternary)), 56.1, 56.0 ( $-\text{OCH}_3$ ), 41.3, 33.7 (piperidine-C), 25.9 ( $-\text{CH}_2-$ ).

### 3.42. 1-(2-(((3-(*p*-tolyl)isoxazol-5-yl)methyl)thio)pyrimidin-4-yl) piperidin-4-ol (**8f**)

Thick yellow mass; 66% yield;  $^1\text{H}$  NMR ( $\text{CDCl}_3$ , 500 MHz):  $\delta$  7.98 (d,  $J = 6.0$  Hz, 1H, pyrimidine-H), 7.64 (d,  $J = 8.0$  Hz, 2H,  $-\text{C}_6\text{H}_4$ ), 7.23 (d,  $J = 8.0$  Hz, 2H,  $-\text{C}_6\text{H}_4$ ), 6.52 (s, 1H, isoxazole-H), 6.22 (d,  $J = 6.5$  Hz, 1H, pyrimidine-H), 4.40 (s, 2H,  $-\text{CH}_2-$ ), 4.05–3.89 (m, 4H, piperidine-H (3H) and OH (1H)), 3.36–3.22 (m, 2H, piperidine-H), 2.37 (s, 3H,  $-\text{CH}_3$ ), 1.97–1.83 (m, 2H, piperidine-H), 1.60–1.43 (m, 2H, piperidine-H);  $^{13}\text{C}$  NMR ( $\text{CDCl}_3$ , 126 MHz):  $\delta$  171.0, 168.7, 162.6, 160.8, 155.9, 140.1, 129.6, 126.7, 126.3, 100.4, 99.1 (Ar-C), 67.2 (piperidine-C (quaternary)), 41.3, 33.7 (piperidine-C), 25.9 ( $-\text{CH}_2-$ ), 21.5 ( $-\text{CH}_3$ ); LCMS (ESI):  $m/z$  calcd. for  $\text{C}_{20}\text{H}_{22}\text{N}_4\text{O}_2\text{S}$ : 382.4793, found = 383.1446  $[\text{M} + \text{H}]^+$ .

### 3.43. Cell Viability Assay

First,  $2 \times 10^3$  MCF-7 cells were cultured in MEM, or Leibovitz's L-15 medium enriched with 2% FBS, and maintained in a humidified atmosphere of 5%  $\text{CO}_2$  at 37 °C [44]. DMSO-dissolved compounds were kept as a stock solution and diluted with a cell culture medium to the desired concentration. Cancer cells ( $4 \times 10^3$ ) were grown overnight in 96-well plates, cultured, and treated with triazoles/isoxazoles at 0, 0.01, 0.1, 10, 100, and 1000  $\mu\text{M}$  concentrations for 72 h. The inhibitory effect of the compounds was assessed using the Alamar Blue reagent.

### 3.44. Molecular Docking Studies

The Scripps Research Institute's AutoDock4 tools (ADT) v1.5.6 [45] were used to determine the docking studies. The co-crystal structure of HDAC7 (PDB ID: 3ZNR) was obtained from the Protein Data Bank (PDB), and the structure was downloaded in PDB format for further analysis. Then, ligand structures, including the novel isoxazole (**7d**), triazole (**5h**) analogues, and the co-crystal ligand, were prepared. The ligand structures were built and optimized using molecular modeling software (Discovery Studio & Avogadro) [46] to ensure proper geometry and energy minimization [47–53]. The ligand structures were saved in the appropriate file format (PDB) for AutoDock4 Tools. Later, the HDAC7 crystal structure (PDB ID: 3ZNR) was loaded into AutoDock4 Tools, and water molecules, co-factors, and other non-essential entities were removed to isolate the protein of interest. The protein structure was prepared by adding polar hydrogen atoms and assigning Kollman charges. A grid box was defined around the HDAC7 to guide the docking simulation with dimensions  $60\text{Å} \times 60\text{Å} \times 70\text{Å}$  with a spacing of  $1\text{Å}$ . Then, docking was initiated by selecting macromolecule (HDAC7) and ligand (**7d**) with a genetic algorithm as the search parameter was set, and the output file was the Lamarckian default parameter file. Initially, 150 were randomly placed individually with a maximum number of  $2.5 \times 10^6$  energy evaluations having a mutation rate of 0.02 and crossover rate of 0.80, and 10 docking runs were performed for compound **7d**. Similarly, all steps were performed for the compound **5h** and co-crystal ligand (TMP269). Visualization of docking results was examined using Discovery Studio [54], pymol [55], and UCSF chimera 1.16 [56].

## 4. Conclusions

In conclusion, the novel thiouracil-tethered triazole-based compounds were synthesized by both conventional and electrolytic methods. The synthesis of 1,2,3-triazoles via electrochemical oxidation provided a good yield and was found to be highly useful for synthesizing bioactive molecules based on triazoles. Moreover, the thiouracil-tethered isoxazole-based compounds were synthesized and presented a better procedure to prepare at a high yield. Additionally, we offered a unique green protocol for synthesizing isoxazole- and triazole-based compounds in the presence of the thiouracil group. Herein, in a target-based study, we further examined the discovered compound's mode of action *in silico* by considering the reference co-crystal structure of HDAC and its inhibitors and showed that the newly synthesized compounds could mimic HDACis in BC cells. The lead compound, such as **6l** or **5h**, could effectively inhibit BC cell proliferation with a lower  $\text{IC}_{50}$  value. Furthermore, we discovered through an *in silico* investigation that these

lead compounds could bind to the catalytic areas of HDAC. In conclusion, we provided a new chemical entity bearing triazole, isoxazole, and thiouracil moiety, which might target HDAC in BC cells.

**Supplementary Materials:** The following supporting information can be downloaded at <https://www.mdpi.com/article/10.3390/molecules28135254/s1>. Supplementary data contains NMR, LCMS, and IC<sub>50</sub> values of newly synthesized compounds (5a–l), (6a–l), (7a–f), and (8a–f).

**Author Contributions:** D.V., Z.X., A.R., A.M., S.B., N.P.K., S.L.G. and B.B., conceptualization, methodology, formal analysis, and writing; V.P., P.E.L. and B.B., conceptualization, methodology, software, data curation, original draft, validation, writing, and editing. All authors have read and agreed to the published version of the manuscript.

**Funding:** This work was supported by Vision Group on Science and Technology (CESEM) and the Government of Karnataka. This work was also supported by the Shenzhen Key Laboratory of Innovative Oncotherapeutics (ZDSYS20200820165400003) (Shenzhen Science and Technology Innovation Commission), China; the Shenzhen Development and Reform Commission Subject Construction Project ([2017]1434), China; the Overseas Research Cooperation Project (HW2020008) (Tsinghua Shenzhen International Graduate School), China; the Tsinghua University Stable Funding Key Project (WDZC20200821150704001); the Shenzhen Bay Laboratory (21310031), China; and TBSI Faculty Start-up Funds, China. Thanks to KSTePS (DST PhD Fellowship), Karnataka, for funding D.V. and A.R.

**Institutional Review Board Statement:** Not applicable.

**Informed Consent Statement:** Not applicable.

**Data Availability Statement:** All data are freely available within this article.

**Conflicts of Interest:** The authors declare no conflict of interest.

**Sample Availability:** Samples of the compounds are not available from the authors.

## References

1. Li, Y.; Seto, E. HDACs and HDAC Inhibitors in Cancer Development and Therapy. *Cold Spring Harb. Perspect. Med.* **2016**, *6*, a026831. [[CrossRef](#)] [[PubMed](#)]
2. Eichner, L.J.; Curtis, S.D.; Brun, S.N.; McGuire, C.K.; Gushterova, I.; Baumgart, J.T.; Trefts, E.; Ross, D.S.; Rymoff, T.J.; Shaw, R.J. HDAC3 Is Critical in Tumor Development and Therapeutic Resistance in *Kras* -Mutant Non-Small Cell Lung Cancer. *Sci. Adv.* **2023**, *9*, eadd3243. [[CrossRef](#)] [[PubMed](#)]
3. Wang, J.; Zhong, F.; Li, J.; Yue, H.; Li, W.; Lu, X. The Epigenetic Factor CHD4 Contributes to Metastasis by Regulating the EZH2/ $\beta$ -Catenin Axis and Acts as a Therapeutic Target in Ovarian Cancer. *J. Transl. Med.* **2023**, *21*, 38. [[CrossRef](#)] [[PubMed](#)]
4. Wattanathamsan, O.; Chantaravisoot, N.; Wongkongkathep, P.; Kungsukool, S.; Chetprayoon, P.; Chanvorachote, P.; Vinayanuwattikun, C.; Pongrakhananon, V. Inhibition of Histone Deacetylase 6 Destabilizes ERK Phosphorylation and Suppresses Cancer Proliferation via Modulation of the Tubulin Acetylation-GRP78 Interaction. *J. Biomed. Sci.* **2023**, *30*, 4. [[CrossRef](#)] [[PubMed](#)]
5. Renoir, J.-M.; Marsaud, V.; Lazennec, G. Estrogen Receptor Signaling as a Target for Novel Breast Cancer Therapeutics. *Biochem. Pharmacol.* **2013**, *85*, 449–465. [[CrossRef](#)] [[PubMed](#)]
6. Milazzo, G.; Mercatelli, D.; Di Muzio, G.; Triboli, L.; De Rosa, P.; Perini, G.; Giorgi, F.M. Histone Deacetylases (HDACs): Evolution, Specificity, Role in Transcriptional Complexes, and Pharmacological Actionability. *Genes* **2020**, *11*, 556. [[CrossRef](#)]
7. Seto, E.; Yoshida, M. Erasers of Histone Acetylation: The Histone Deacetylase Enzymes. *Cold Spring Harb. Perspect. Biol.* **2014**, *6*, a018713. [[CrossRef](#)]
8. Park, S.-Y.; Kim, J.-S. A Short Guide to Histone Deacetylases Including Recent Progress on Class II Enzymes. *Exp. Mol. Med.* **2020**, *52*, 204–212. [[CrossRef](#)]
9. Ahrens, S.; Geissler, B.; Satchell, K.J. Identification of a His-Asp-Cys Catalytic Triad Essential for Function of the Rho Inactivation Domain (RID) of *Vibrio cholerae* MARTX Toxin. *J. Biol. Chem.* **2013**, *288*, 1397–1408. [[CrossRef](#)] [[PubMed](#)]
10. Daško, M.; de Pascual-Teresa, B.; Ortín, I.; Ramos, A. HDAC Inhibitors: Innovative Strategies for Their Design and Applications. *Molecules* **2022**, *27*, 715. [[CrossRef](#)]
11. Kerek, E.; Yoon, K.E.; Luo, S.; Chen, J.Y.; Valencia, R.; Julien, O.; Waskiewicz, A.J.; Hubbard, B.P. A Conserved Acetylation Switch Enables Pharmacological Control of Tubby-like Protein Stability. *J. Biol. Chem.* **2021**, *296*, 100073. [[CrossRef](#)]
12. Tang, J.; Yan, H.; Zhuang, S. Histone Deacetylases as Targets for Treatment of Multiple Diseases. *Clin. Sci.* **2013**, *124*, 651–662. [[CrossRef](#)]
13. Hadden, M.; Advani, A. Histone Deacetylase Inhibitors and Diabetic Kidney Disease. *Int. J. Mol. Sci.* **2018**, *19*, 2630. [[CrossRef](#)]

14. Negmeldin, A.T.; Padige, G.; Bieliauskas, A.V.; Pflum, M.K.H. Structural Requirements of HDAC Inhibitors: SAHA Analogues Modified at the C2 Position Display HDAC6/8 Selectivity. *ACS Med. Chem. Lett.* **2017**, *8*, 281–286. [CrossRef]
15. Banerjee, N.S.; Moore, D.W.; Broker, T.R.; Chow, L.T. Vorinostat, a Pan-HDAC Inhibitor, Abrogates Productive HPV-18 DNA Amplification. *Proc. Natl. Acad. Sci. USA* **2018**, *115*, E11138–E11147. [CrossRef]
16. Chifotides, H.T.; Bose, P.; Verstovsek, S. Givinostat: An Emerging Treatment for Polycythemia Vera. *Expert Opin. Investig. Drugs* **2020**, *29*, 525–536. [CrossRef]
17. Sharma, V.; Koul, N.; Joseph, C.; Dixit, D.; Ghosh, S.; Sen, E. HDAC Inhibitor, Scriptaid, Induces Glioma Cell Apoptosis through JNK Activation and Inhibits Telomerase Activity. *J. Cell. Mol. Med.* **2010**, *14*, 2151–2161. [CrossRef] [PubMed]
18. Arts, J.; King, P.; Marien, A.; Floren, W.; Beliën, A.; Janssen, L.; Noëlle, I.; Roux, B.; Decrane, L.; Gilissen, R.; et al. JNJ-26481585, a Novel Second-Generation Oral Histone Deacetylase Inhibitor, Shows Broad-Spectrum Preclinical Antitumoral Activity. *Clin. Cancer Res.* **2009**, *15*, 6841–6851. [CrossRef] [PubMed]
19. Fleming, C.L.; Ashton, T.D.; Gaur, V.; McGee, S.L.; Pfeffer, F.M. Improved Synthesis and Structural Reassignment of MC1568: A Class IIa Selective HDAC Inhibitor. *J. Med. Chem.* **2014**, *57*, 1132–1135. [CrossRef] [PubMed]
20. Qu, X.; Ying, H.; Wang, X.; Kong, C.; Zhou, X.; Wang, P.; Zhu, H. Histone Deacetylase Inhibitor MC1293 Induces Latent HIV-1 Reactivation by Histone Modification in Vitro Latency Cell Lines. *Curr. HIV Res.* **2013**, *11*, 24–29. [PubMed]
21. Amengual, J.E.; Lue, J.K.; Ma, H.; Lichtenstein, R.; Shah, B.; Cremers, S.; Jones, S.; Sawas, A. First-In-Class Selective HDAC6 Inhibitor (ACY-1215) Has a Highly Favorable Safety Profile in Patients with Relapsed and Refractory Lymphoma. *Oncologist* **2021**, *26*, e184–e366. [CrossRef]
22. Jo, S.; Kim, J.-H.; Lee, J.; Park, Y.; Jang, J. Azumamides A-E: Isolation, Synthesis, Biological Activity, and Structure–Activity Relationship. *Molecules* **2022**, *27*, 8438. [CrossRef]
23. Zhang, S.; Fujita, Y.; Matsuzaki, R.; Yamashita, T. Class I Histone Deacetylase (HDAC) Inhibitor CI-994 Promotes Functional Recovery Following Spinal Cord Injury. *Cell Death Dis.* **2018**, *9*, 460. [CrossRef]
24. Leus, N.G.J.; van der Wouden, P.E.; van den Bosch, T.; Hooghiemstra, W.T.R.; Ourailidou, M.E.; Kistemaker, L.E.M.; Bischoff, R.; Gosens, R.; Haisma, H.J.; Dekker, F.J. HDAC 3-Selective Inhibitor RGFP966 Demonstrates Anti-Inflammatory Properties in RAW 264.7 Macrophages and Mouse Precision-Cut Lung Slices by Attenuating NF- $\kappa$ B P65 Transcriptional Activity. *Biochem. Pharmacol.* **2016**, *108*, 58–74. [CrossRef]
25. Wu, C.-P.; Lusvardi, S.; Wang, J.-C.; Hsiao, S.-H.; Huang, Y.-H.; Hung, T.-H.; Ambudkar, S.V. The Selective Class IIa Histone Deacetylase Inhibitor TMP195 Resensitizes ABCB1- and ABCG2-Overexpressing Multidrug-Resistant Cancer Cells to Cytotoxic Anticancer Drugs. *Int. J. Mol. Sci.* **2019**, *21*, 238. [CrossRef]
26. Ashwini, N.; Garg, M.; Mohan, C.D.; Fuchs, J.E.; Rangappa, K.S.; Anusha, S.; Swaroop, T.R.; Rakesh, K.S.; Kanojia, D.; Madan, V.; et al. Synthesis of 1,2-Benzisoxazole Tethered 1,2,3-Triazoles That Exhibit Anticancer Activity in Acute Myeloid Leukemia Cell Lines by Inhibiting Histone Deacetylases, and Inducing P21 and Tubulin Acetylation. *Bioorganic Med. Chem.* **2015**, *23*, 6157–6165. [CrossRef] [PubMed]
27. Ding, C.; Li, D.; Wang, Y.; Han, S.; Gao, C.; Tan, C.; Jiang, Y. Discovery of ErbB/HDAC Inhibitors by Combining the Core Pharmacophores of HDAC Inhibitor Vorinostat and Kinase Inhibitors Vandetanib, BMS-690514, Neratinib, and TAK-285. *Chin. Chem. Lett.* **2017**, *28*, 1220–1227. [CrossRef]
28. Mai, A.; Massa, S.; Rotili, D.; Simeoni, S.; Ragno, R.; Botta, G.; Nebbioso, A.; Miceli, M.; Altucci, L.; Brosch, G. Synthesis and Biological Properties of Novel, Uracil-Containing Histone Deacetylase Inhibitors. *J. Med. Chem.* **2006**, *49*, 6046–6056. [CrossRef]
29. Bernards, R.; Epping, M.; Wang, L. Combined Use of Prame Inhibitors and Hdac Inhibitors. U.S. Patent 7,928,081, 19 April 2011. Available online: <https://patents.google.com/patent/EP2392677A2/en> (accessed on 20 February 2023).
30. Shen, S.; Hadley, M.; Ustinova, K.; Pavlicek, J.; Knox, T.; Noonepalle, S.; Moreno, I.B.; Zimprich, C.; Zhang, G.-P.; Robers, M.B.; et al. Discovery of a New Isoxazole-3-Hydroxamate-Based Histone Deacetylase 6 Inhibitor SS-208 with Antitumor Activity in Syngeneic Melanoma Mouse Models. *J. Med. Chem.* **2019**, *62*, 8557–8577. [CrossRef] [PubMed]
31. Cho, J.W.; Choi, S.R.; Hwang, S.G.; Cho, K.C.; Bae, S.J.; Koo, T.S. Isoxazole Derivatives and Use Thereof, WO2007078113A1, WIPO (PCT). Available online: <https://patents.google.com/patent/WO2007078113A1/en> (accessed on 20 February 2023).
32. Anusha, S.; Cp, B.; Mohan, C.D.; Mathai, J.; Rangappa, S.; Mohan, S.; Chandra, S.M.; Paricharak, S.; Mervin, L.; Fuchs, J.E.; et al. A Nano-MgO and Ionic Liquid-Catalyzed “Green” Synthesis Protocol for the Development of Adamantyl-Imidazo-Thiadiazoles as Anti-Tuberculosis Agents Targeting Sterol 14 $\alpha$ -Demethylase (CYP51). *PLoS ONE* **2015**, *10*, e0139798. [CrossRef]
33. Basappa; Sugahara, K.; Thimmaiah, K.N.; Bid, H.K.; Houghton, P.J.; Rangappa, K.S. Anti-Tumor Activity of a Novel HS-Mimetic-Vascular Endothelial Growth Factor Binding Small Molecule. *PLoS ONE* **2012**, *7*, e39444. [CrossRef]
34. Zhang, X.; Huang, P.; Wang, L.-Q.; Chen, S.; Basappa, B.; Zhu, T.; Lobie, P.E.; Pandey, V. Inhibition of BAD-Ser99 Phosphorylation Synergizes with PARP Inhibition to Ablate PTEN-Deficient Endometrial Carcinoma. *Cell Death Dis.* **2022**, *13*, 558. [CrossRef]
35. Comşa, Ş.; Cîmpean, A.M.; Raica, M. The Story of MCF-7 Breast Cancer Cell Line: 40 Years of Experience in Research. *Anticancer Res.* **2015**, *35*, 3147–3154.
36. Levenson, A.S.; Jordan, V.C. MCF-7: The first hormone-responsive breast cancer cell line. *Cancer Res.* **1997**, *57*, 3071–3078.
37. Lobera, M.; Madauss, K.P.; Pohlhaus, D.T.; Wright, Q.G.; Trocha, M.; Schmidt, D.R.; Baloglu, E.; Trump, R.P.; Head, M.S.; Hofmann, G.A.; et al. Selective Class IIa Histone Deacetylase Inhibition via a Nonchelating Zinc-Binding Group. *Nat. Chem. Biol.* **2013**, *9*, 319–325. [CrossRef]



38. Kim, N.Y.; Vishwanath, D.; Xi, Z.; Nagaraja, O.; Swamynayaka, A.; Kumar Harish, K.; Basappa, S.; Madegowda, M.; Pandey, V.; Sethi, G.; et al. Discovery of Pyrimidine- and Coumarin-Linked Hybrid Molecules as Inducers of JNK Phosphorylation through ROS Generation in Breast Cancer Cells. *Molecules* **2023**, *28*, 3450. [CrossRef] [PubMed]
39. Pinheiro, L.C.S.; Feitosa, L.M.; Gandi, M.O.; Silveira, F.F.; Boechat, N. The Development of Novel Compounds against Malaria: Quinolines, Triazolopyridines, Pyrazolopyridines and Pyrazolopyrimidines. *Molecules* **2019**, *24*, 4095. [CrossRef]
40. Khazir, J.; Pilcher, L.A.; Riley, D.L.; Chashoo, G. Design and Synthesis of Sulphonyl Acetamide Analogues of Quinazoline as Anticancer Agents. *Med. Chem. Res.* **2020**, *29*, 916–925. [CrossRef]
41. He, H.; Wang, W.; Zhou, Y.; Xia, Q.; Ren, Y.; Feng, J.; Peng, H.; He, H.; Feng, L. Rational Design, Synthesis and Biological Evaluation of 1,3,4-Oxadiazole Pyrimidine Derivatives as Novel Pyruvate Dehydrogenase Complex E1 Inhibitors. *Bioorg. Med. Chem.* **2016**, *24*, 1879–1888. [CrossRef]
42. Shanmugasundaram, M.; Senthilvelan, A.; Kore, A.R. Highly Regioselective 1,3-Dipolar Cycloaddition of 3'-O-Propargyl Guanosine with Nitrile Oxide: An Efficient Method for the Synthesis of Guanosine Containing Isoxazole Moiety. *Tetrahedron Lett.* **2020**, *61*, 152464. [CrossRef] [PubMed]
43. Chappie, T.A.; Helal, C.J.; Kormos, B.L.; Tuttle, J.B.; Verhoest, P.R. Imidazo-Triazine Derivatives as Pde10 Inhibitors, WO2014177977A1, WIPO (PCT). Available online: <https://patents.google.com/patent/WO2014177977A1/en> (accessed on 22 February 2023).
44. Basappa, B.; Chumadathil Pookunoth, B.; Shinduvalli Kempasiddegowda, M.; Knchugarakoppal Subbegowda, R.; Lobie, P.E.; Pandey, V. Novel Biphenyl Amines Inhibit Oestrogen Receptor (ER)- $\alpha$  in ER-Positive Mammary Carcinoma Cells. *Molecules* **2021**, *26*, 783. [CrossRef] [PubMed]
45. Huey, R.; Morris, G.M.; Olson, A.J.; Goodsell, D.S. A Semiempirical Free Energy Force Field with Charge-Based Desolvation. *J. Comput. Chem.* **2007**, *28*, 1145–1152. [CrossRef] [PubMed]
46. Hanwell, M.D.; Curtis, D.E.; Lonie, D.C.; Vandermeersch, T.; Zurek, E.; Hutchison, G.R. Avogadro: An Advanced Semantic Chemical Editor, Visualization, and Analysis Platform. *J. Cheminform.* **2012**, *4*, 17. [CrossRef]
47. Basappa; Kavitha, C.V.; Rangappa, K.S. Simple and an efficient method for the synthesis of 1-[2-dimethylamino-1-(4-methoxyphenyl)-ethyl]-cyclohexanol hydrochloride: (+/-) venlafaxine racemic mixtures. *Bioorg. Med. Chem. Lett.* **2004**, *14*, 3279–3281. [CrossRef]
48. Kanchugarakoppal, S.R.; Basappa. New cholinesterase inhibitors: Synthesis and structure-activity relationship studies of 1,2-benzisoxazole series and novel imidazolyl-d 2-isoxazolines. *J. Phys. Organ. Chem.* **2005**, *18*, 773–778.
49. Fongmoon, D.; Shetty, A.K.; Basappa Yamada, S.; Sugiura, M.; Kongtawelert, P.; Sugahara, K. Chondroitinase-mediated degradation of rare 3-O-sulfated glucuronic acid in functional oversulfated chondroitin sulfate K and E. *J. Biol. Chem.* **2007**, *282*, 36895–36904. [CrossRef]
50. Blanchard, V.; Chevalier, F.; Imbert, A.; Leeflang, B.R.; Basappa Sugahara, K.; Kamerling, J.P. Conformational studies on five octasaccharides isolated from chondroitin sulfate using NMR spectroscopy and molecular modeling. *Biochemistry* **2007**, *46*, 1167–1175. [CrossRef]
51. Anusha, S.; Mohan, C.D.; Ananda, H.; Baburajeev, C.P.; Rangappa, S.; Mathai, J.; Fuchs, J.E.; Li, F.; Shanmugam, M.K.; Bender, A.; et al. Adamantyl-tethered-biphenylic compounds induce apoptosis in cancer cells by targeting Bcl homologs. *Bioorg. Med. Chem. Lett.* **2016**, *26*, 1056–1060. [CrossRef]
52. Sulaiman, N.B.; Mohan, C.D.; Basappa, S.; Pandey, V.; Rangappa, S.; Bharathkumar, H.; Kumar, A.P.; Lobie, P.E.; Rangappa, K.S. An azaspirane derivative suppresses growth and induces apoptosis of ER-positive and ER-negative breast cancer cells through the modulation of JAK2/STAT3 signaling pathway. *Int. J. Oncol.* **2016**, *49*, 1221–1229. [CrossRef]
53. Nirvanappa, A.C.; Mohan, C.D.; Rangappa, S.; Ananda, H.; Sukhorukov, A.Y.; Shanmugam, M.K.; Sundaram, M.S.; Nayaka, S.C.; Girish, K.S.; Chinnathambi, A.; et al. Novel Synthetic Oxazines Target NF- $\kappa$ B in Colon Cancer In Vitro and Inflammatory Bowel Disease In Vivo. *PLoS ONE* **2016**, *11*, e0163209, Erratum in *PLoS ONE* **2017**, *12*, e0175659. [CrossRef]
54. BIOVIA Dassault Systèmes. *Discovery Studio Visualizer*, 21.1.0.20298; Dassault Systèmes: San Diego, CA, USA, 2020.
55. Schrödinger, L.L.C.; DeLano, W. PyMOL. 2020. Available online: <http://www.pymol.org/pymol> (accessed on 15 February 2022).
56. Pettersen, E.F.; Goddard, T.D.; Huang, C.C.; Couch, G.S.; Greenblatt, D.M.; Meng, E.C.; Ferrin, T.E. UCSF Chimera—A Visualization System for Exploratory Research and Analysis. *J. Comput. Chem.* **2004**, *25*, 1605–1612. [CrossRef] [PubMed]

**Disclaimer/Publisher's Note:** The statements, opinions and data contained in all publications are solely those of the individual author(s) and contributor(s) and not of MDPI and/or the editor(s). MDPI and/or the editor(s) disclaim responsibility for any injury to people or property resulting from any ideas, methods, instructions or products referred to in the content.